Developing a novel diagnostic solution for Inflammatory Bowel Disease (IBD)

Thesis Project by Sithma Gunawardena

University of Sydney Engineering and Technology Precinct & The Charles Perkins Centre

Supervised by Dr Yogambha Ramaswamy
Co-supervised by Dr Belal Chami & Dr Syamak Farajikhah

THE UNIVERSITY OF SYDNEY

A thesis submitted in fulfilment of the requirements of the degree of Bachelor of Engineering (Honours)

School of Biomedical Engineering
The University of Sydney

November 2025

Abstract

Inflammatory bowel disease (IBD) is a difficult and unpredictable condition that many people live with, and its episodic, painful flares have a major impact on quality of life, making regular monitoring essential. Current monitoring tools, such as endoscopy and laboratory faecal calprotectin, are safe and effective but they are also costly, time-consuming and inconvenient, which limits how often they can be used. In this thesis, we explore a home-compatible testing approach that uses myeloperoxidase (MPO), an enzyme released by activated neutrophils, as a more direct biomarker of intestinal inflammation. Instead of relying on antibody-based protein mass measurements, MPO activity is translated into an electrical signal by coupling its oxidant products to a simple redox probe on an electrode surface. In controlled experiments, increasing MPO-derived oxidant led to a clear, dose-dependent drop in electrochemical current, with an estimated limit of detection of 2.4 µM taurine chloramine (TauCl) and a limit of quantification of 7.9 µM TauCl at 1 µg/mL MPO, demonstrating sensitivity in the low micromolar range without complex laboratory infrastructure. These results provide a proof-of-concept for an MPO-based sensor that could ultimately be integrated into disposable electrodes and portable readers, forming the basis of a non-invasive home testing kit to help patients self-monitor their IBD activity more frequently and conveniently.

Acknowledgements

I would like to first express my gratitude to my supervisors Dr. Belal Chami and Dr Syamak Farajikhah for their guidance and support throughout this year. Your mentorship has made a lasting impression on me and I'm grateful I was able to be involved in a project so impactful.

I would also like to thank the wider group at the J03 Engineering and Technology Precinct, especially Azadeh Abdi and Aylar Eslami. Thank you for the shared laughter and being so eager to help. Azadeh, I am particularly grateful for her knowledge and expertise in my field with ample resources from her own research to help me finish my own thesis.

Additionally, I would also like to extend a thank you to all the previous honours students whose hard work laid the groundwork for this project.

Finally, I would like to thank my family namely my mother, my sister Piumi and my brother-in-law, Michael, who all gave me unwavering support during stressful times.

Declaration

- I conducted the literature review that provides the scientific and clinical context for this thesis, including the discussion of inflammatory bowel disease biomarkers, neutrophil-derived markers and electrochemical biosensing approaches.
- I contributed to the overall study design and experimental plan for developing an electrochemical assay for myeloperoxidase (MPO) activity, in consultation with my supervisors.
- I prepared all reagents described in this thesis (including phosphate-buffered saline, hypochlorous acid/bleach and taurine solutions), and carried out the chemical calibration experiments to relate HOCl/TauCl dose to electrochemical signal.
- I performed the electrochemical measurements reported in this thesis (including cyclic voltammetry and related techniques) using screen-printed and/or conventional electrodes, and optimised the measurement parameters under supervisor guidance.
- I wrote the code used for data processing, analysis and figure generation (e.g. importing raw potentiostat output, extracting peak currents, constructing calibration curves and calculating limits of detection/quantification) using OriginPro.
- I analysed the experimental results, interpreted the model performance and assay behaviour in light of current literature, and drafted the results and discussion chapters.
- I wrote and revised all chapters of this thesis, integrating supervisor feedback on structure, clarity and scientific accuracy.

The above represents an accurate summary of my contribution to this thesis.

Sithma Gunawardena (Student) 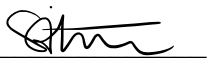

Dr Yogambha Ramaswamy (Supervisor) 

List of figures and tables

Table of Contents

Chapter 1: Introduction

1.1 Inflammatory Bowel Disease: A clinical overview

Inflammatory Bowel Disease (IBD) is a chronic, relapsing inflammation of the gastrointestinal tract comprising two varieties named Crohn's Disease (CD) and Ulcerative Colitis (UC) [1]. IBD arises when a dysregulated immune response targets commensal microbiota in genetically susceptible individuals who encounter environmental triggers such as diet, infections, or medications [2]. Recent research shows that incidence and prevalence of IBD continue to rise globally across all ages, with increasing paediatric cases and a substantial proportion of patients aged 65 years and older [1], [2], [3]. The resulting long disease course imposes significant clinical and economic burdens, underscoring the need to optimise monitoring and treatment strategies to limit societal and healthcare impact [3], [4].

Clinically, IBD alternates between unpredictable flares and remission. Typical flare symptoms include abdominal pain, diarrhoea, weight loss, and fatigue [5]. Pathologically, recruited neutrophils and macrophages damage the mucosa through cytokine release and oxidative chemistry, producing variable symptom severity with little warning. This volatility makes it both clinically essential and technically difficult to monitor the disease objectively and in a timely manner.

CD and UC are distinguished by the distribution and the depth of inflammation [6]. CD can affect any part of the gastrointestinal tract and most often the terminal ileum and colon, and it is characterised by patchy, transmural inflammation that increases the risk of strictures, fistulae, and extraintestinal manifestations [7]. UC is confined to the colon and rectum, typically, it begins at the rectum, and it is characterized by continuous mucosal inflammation with risks including bleeding and long-term progression to colorectal cancer [7]

Given these patterns of inflammation, first-line therapies typically include aminosalicylates, corticosteroids, and immunomodulators to control symptoms and suppress inflammation. Many patients fail to respond or lose response over time, and adverse effects are common, leaving persistent disease activity [8]. Biologic and other advanced therapies have reduced surgery rates and improved control, but they are costly, and a sizeable fraction of patients experience primary or secondary non-response [8]. A faster, more effective, and reliable diagnosis of IBD can

significantly improve patients' quality of life by reducing the need for repeated visits to general practitioners and equipping them with tools to monitor their condition independently.

IBD treatment focuses on achieving remission and improving quality of life, as there is no cure. STRIDE-II guidelines emphasise the main long-term targets are clinical remission, endoscopic healing, and restoration of quality of life [1]. A meta-analysis by Jayasooriya et al. [9] identified that delayed diagnosis led to prolonged symptoms, unnecessary investigations, higher risk of complications such as strictures, fissues and the need for surgery. The development of rapid, point-of-care diagnostic technologies is an effective strategy to mitigate the financial burden and avoid delays associated with current testing methods, and consequently by reduce patient complications.

Recent research [10], [11], [12] has seen the advantage of understanding Neutrophils, an innate immune response due to the stimulation of the immune system. These neutrophils cause the dysregulation of the immune system and neutrophil-derived biomarkers such as fecal calprotectin (fCal) and fecal myeloperoxidase (fMPO) have been used in the diagnostic processes as neutrophil effector molecules that can be measured directly at the site of inflammation. Myeloperoxidase (MPO) is a proximate readout because neutrophils release it during degranulation into inflamed mucosa and the lumen, providing a direct signal of active neutrophilic inflammation in IBD. The key purpose of this thesis project is to use fMPO's electrochemical behaviour for its advantage in developing a novel miniaturised tool to detect IBD. While developing an effective device can be time consuming requiring conceptualisation, phototyping, testing and iterative redesign, this thesis provides a conceptual design which has the potential to evolve into a fully-fledged diagnostic device.

MPO has shown promise in previous studies as a biomarker for intestinal inflammation [4]. Despite its potential, fMPO is not widely used in clinical practice due to a lack of robust, accessible detection platforms. Existing techniques are laboratory-dependent and provide limited point-of-care utility. Chemiluminescence-based detection (Myeloperoxidase Luminol Reaction - MPOLR) has been explored but lacks quantification precision and practical translation into a low-cost, home-based system [1].

There is an unmet need for a portable, non-invasive, quantitative diagnostic tool that can detect fecal MPO accurately at the point-of-care. Existing gold-standard biomarkers like calprotectin and

lactoferrin, while clinically accepted, do not fully capture the dynamic inflammatory profile nor are they well suited for real-time at-home testing [13]

1.2 Myeloperoxidase: origin, structure and role in IBD

MPO is a dimeric glycoprotein of about 150 kDa, comprising two identical protomers linked by a disulfide bridge as shown by *Fig 1*. Each protomer contains a 59 kDa heavy chain and a 14.5 kDa light chain and carries a heme prosthetic group essential for catalysis. In human MPO the heme is covalently tethered to the protein, while the heavy chain is stabilised by multiple disulfide bonds and N-linked glycans. This architecture shows exceptional conformational and chemical stability, allowing MPO to retain activity under acidic, oxidising conditions typically in inflamed tissue and within fecal matrices [14], [15]

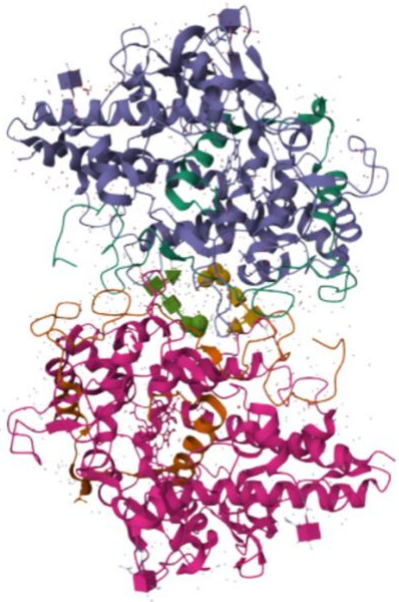

Figure 1. *Crystal structure of human myeloperoxidase [15]*

At the catalytic level, MPO uses hydrogen peroxide to generate high-valent oxo–ferryl intermediates (Compounds I and II), which drive two related reaction cycles as shown by *Fig 2*. In the halogenation cycle, Compound I oxidises physiological anions to generate oxidants, most prominently hypochlorous acid (HOCl) from chloride and hypothiocyanous acid from thiocyanate. In the peroxidase cycle, MPO oxidises a broad range of organic substrates to radicals, amplifying

oxidative signalling. These pathways produce specific, measurable species and redox transitions that analytical methods can exploit [16]

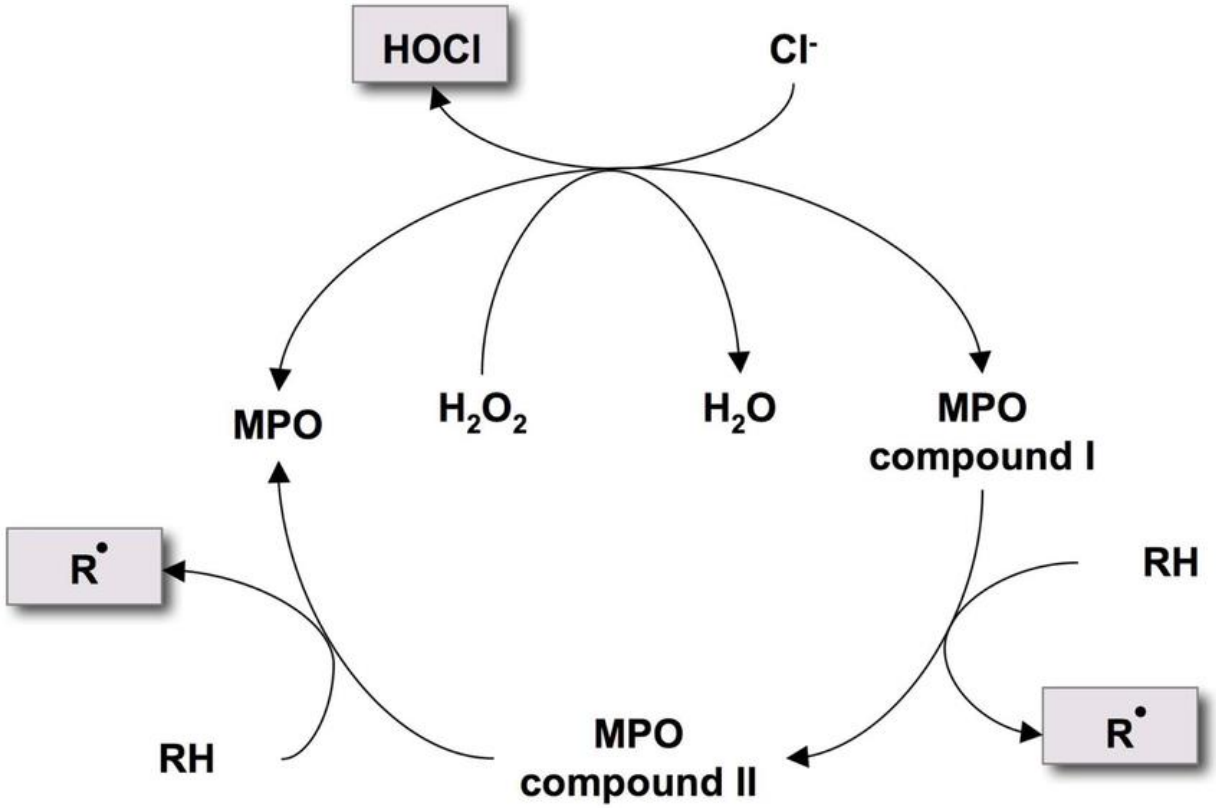

***Figure 2**. Halogenation and peroxidase cycle of MPO [16]*

MPO is practical to assay because its heme centre has distinctive spectral and electrochemical signatures. Activity can be quantified with chromogenic substrates, chemiluminescence, or electrochemical methods that convert either heme redox changes or product formation into an electrical signal. MPO remains stable in stool, which supports fecal testing and fits real-time, point-of-care monitoring [14]

1.3 Research gap and research problem

As aforementioned, modern IBD diagnostics are costly, invasive and introduce significant risks as a result of delays to treatment, there is a need to develop rapid, reliable and accurate, non-invasive technology for real time diagnostics of IBD [17]. The existing tools are primarily designed to be used by clinicians and technicians in laboratory settings. However, there is a growing need for home-based, self-monitoring tools that empower patients to track their condition more effectively.

Such tools could significantly reduce the frequency of hospital visits and reliance on laboratory testing, thereby lowering healthcare costs and minimising delays in care. More importantly, enabling patients to monitor disease activity at home can lead to earlier detection of flares, improved adherence to treatment plans, and enhanced quality of life [18]. By shifting from centralized testing to patient-driven monitoring, this approach has the potential to transform disease management and deliver more personalized, timely intervention. This thesis project is to address that gap utilizing the chemical behaviour of MPO and its structural significance.

1.4 Project Objectives

This project aims to deliver a fast, low-cost electrochemical strategy for quantifying fecal myeloperoxidase that can ultimately support responsive, at-home monitoring of inflammatory bowel disease activity. The core idea is to exploit MPO's generation of HOCl to produce robust electrochemical signals that can be translated into fMPO activity. The endpoint is a validated sensing workflow and an accompanying hardware concept that align with STRIDE II [19] treat-to-target goals for timely, objective assessment of inflammation and early intervention. Within this overarching objective, the work is organised around two main aims. **Identify a diagnostic solution that is fast, reliable, and quantitatively interpretable (A1),** and **provide an electrochemical engineering pathway to miniaturised, home-use diagnostic equipment (A2)**.

1.5 Hypotheses

This study is guided by three interrelated hypotheses that underpin the conceptual design and its potential clinical impact:

Redox–signal coupling

HOCl generated by MPO activity will induce reproducible, concentration-dependent changes in the cyclic voltammetry (CV) response of a reporter redox species on screen-printed electrode (SPE) working electrode. These changes will produce a monotonic calibration function that allows back-calculation of HOCl concentration, and thus MPO activity, over a clinically relevant range.

Matrix translation

Calibration functions established in simple buffer systems using HOCl standards can be translated to stool extracts with acceptable recovery and precision after minimal sample preparation. Under these conditions, electrochemically derived fMPO estimates are expected to show clinically acceptable agreement with a reference assay (e.g., ELISA), within predefined analytical error limits suitable for decision-making in IBD monitoring.

Clinical linkage

Electrochemically measured fMPO concentrations will correlate with validated endoscopic activity indices (e.g. UCEIS or SES-CD) at least as strongly as fecal calprotectin in a validation set. This level of agreement would support the clinical relevance of the electrochemical method and its potential to contribute to STRIDE II-aligned treat-to-target strategies.

1.6 Project aims

Aim 1: Identify a solution to diagnosis that is fast, reliable, and quantifiable

1. Optimise the electrochemical transducer
Engineer and characterise SPE platforms to obtain stable, high signal-to-noise CV readouts. This includes tuning scan parameters, reporter chemistry, and surface preparation to minimise drift, maximise sensitivity to HOCl, and ensure good repeatability.

2. Quantify analytical performance for HOCl and fMPO
Define the linear range, limit of detection, limit of quantification, precision, accuracy, and robustness of the assay for HOCl standards, and then for MPO-derived HOCl. Use these data to establish calibration curves that permit quantitative fMPO estimation from stool extracts.

Aim 2: Provide an electrochemical engineering solution to miniaturise diagnostic equipment

1. Define system requirements for a portable, home-use device
Translate the benchtop protocol into specifications for a miniaturised system by identifying electrical (potentiostat performance, power requirements), mechanical (form factor, robustness), and fluidic/sample-handling requirements compatible with home use.

2. Map a benchtop-to-portable development pathway

Develop a conceptual design for a compact diagnostic platform that integrates the optimised electrochemical transducer, simple sample preparation, and user-friendly readout. Identify components and steps that currently limit size, cost, or usability, and propose engineering solutions that address these constraints, using existing home-use faecal calprotectin platforms such as IBDoc [20] as qualitative benchmarks for feasible sample collection, extraction, and smartphone-based result delivery.

3. Align device concept with user workflow and STRIDE II goals

Outline a realistic at-home workflow (from sample collection to result) that minimises user burden and turnaround time while maintaining analytical performance. Explicitly map how this miniaturised system could support STRIDE II [19] objectives by enabling more frequent, objective assessment of inflammation and timely treatment adjustments

Chapter 2: Literature Review & Diagnostic Context

This chapter provides an overview of the pathophysiology of Inflammatory Bowel Disease (IBD), outlining the underlying mechanisms that contribute to its onset and progression. It then explores current diagnostic approaches, clinical management strategies, and methods used to monitor disease activity. Together, these sections establish the clinical and scientific context for the development of improved diagnostic tools discussed later in the thesis.

2.1 Pathophysiology of IBD: Overview

The pathogenesis of IBD, as revealed by recent research, is marked by the dysregulated recruitment and activation of neutrophils within the intestinal lumen, resulting in the production of pro-inflammatory cytokines and reactive oxygen species (ROS) [8]. In response to microbial and tissue-derived signals, chemokines and cytokines keep "cycling" through an innate immune response, prompting a rapid influx of neutrophils to sites of inflammation. This continuous intestinal damage builds up where oxidative damage from neutrophil products leads to further recruitment of inflammatory signals, leading to progressively more damage [8]. Table I summarises the key molecular and cellular events implicated in the pathogenesis of IBD.

Table I: The key molecular and cellular events implicated in the pathogenesis of IBD.

Key Event	Effect in IBD
Reduced occludin	Increased gut permeability, further immune cell infiltration [11]
Elevated granulocyte colony-stimulating factors (G-CSF/GM-CSF)	Delayed neutrophil apoptosis, accumulation [21], [22]
Neutrophil granule protein release	Tissue damage, chronic inflammation [11]

When neutrophils from the innate immune system enter and build up in the colon, they become activated and release antimicrobial proteins such as MPO, calprotectin, and lactoferrin. These proteins can be measured in stool samples and serve as non-invasive biomarkers of inflammation [22].

Biomarkers derived from the neutrophil axis

Neutrophil products that spill into the lumen are quantifiable in stool and map to disease activity:

- **MPO:** a catalytic enzyme that generates HOCl, reflecting active neutrophil oxidative capacity and correlating with mucosal neutrophil load.
- **Calprotectin:** an S100A8/A9 complex that is highly abundant in neutrophils and serves as a robust abundance marker of neutrophil influx and mucosal inflammation [22]
- **Lactoferrin:** a neutrophil granule glycoprotein that tracks luminal neutrophil presence and tissue injury [22]

Together, these markers capture complementary facets of the same biology: MPO reports enzymatic activity and oxidative potential, whereas calprotectin and lactoferrin primarily report neutrophil mass and degranulation.

2.2 Advances in Understanding Pathogenesis

Both Crohn's disease (CD) and ulcerative colitis (UC) are polygenic. Genome-wide association studies have identified more than 160 susceptibility loci, with roughly one third shared between CD and UC and additional loci specific to each disease (21 to UC and 23 to CD) [23]. This genetic heterogeneity contributes to differences in disease location, behaviour, and treatment response. Composite genetic risk scores can stratify ileal CD, colonic CD, and UC with useful predictive value [23].

Despite genetic complexity, a consistent histological hallmark of active IBD is dense neutrophil infiltration of the intestinal mucosa. Recruitment is driven by epithelial and myeloid chemokines such as CXCL8/IL-8 and CXCL1, complement fragment C5a, and lipid mediators like leukotriene B4. Neutrophils roll on activated endothelium via selectins, achieve firm adhesion through β2-integrins (LFA-1 and Mac-1) engaging ICAM-1, then transmigrate across endothelium and epithelium into crypts, where crypt abscesses form in severe disease [24]. Once in tissue, they degranulate in a tiered fashion: primary (azurophilic) granules release myeloperoxidase, neutrophil elastase, and cathepsin G; secondary (specific) granules release lactoferrin and lysozyme; tertiary (gelatinase) granules release MMP-9 [24], [25]. In parallel, the NADPH oxidase complex generates superoxide that dismutates hydrogen peroxide, which MPO uses with chloride to generate HOCl. Proteases and oxidants together disrupt mucus, tight junctions, and extracellular

matrix, injuring epithelium and microvasculature. Activated neutrophils can also form neutrophil extracellular traps, where chromatin decorated with MPO and proteases is expelled to trap microbes but also propagates thrombosis and matrix degradation in inflamed bowel [10]. Pro-survival cytokines in the IBD milieu delay neutrophil apoptosis and impair efferocytosis, prolonging their residence time and sustaining cytokine and chemokine release. This biology explains why stool biomarkers derived from neutrophil contents differ mechanistically: calprotectin reflects cytosolic release, lactoferrin reflects specific granule secretion, and MPO reflects primary granule degranulation and oxidative burst activity [24], [25].

2.3. IBD Diagnosis

The prevailing model for IBD onset is an abnormal immune response to intestinal microbiota in genetically susceptible individuals exposed to environmental stimuli such as diet, infections, or medications. In predisposed hosts these triggers initiate or reactivate mucosal inflammation that can persist or relapse despite treatment.

As illustrated in *Fig 3*, MPO has dual consequences in inflamed tissue. Beneficially, it supports bacterial killing and can degrade select cytokines. Pathogenically, MPO promotes tissue injury, endothelial dysfunction, thrombosis, and features of autoimmunity. MPO release also drives neutrophil extracellular trap (NET) formation which, while antimicrobial, propagates thrombosis and extracellular matrix breakdown, findings typical of severe IBD. By suppressing neutrophil apoptosis, MPO sustains chemokine and cytokine release that maintains the inflammatory loop [10].

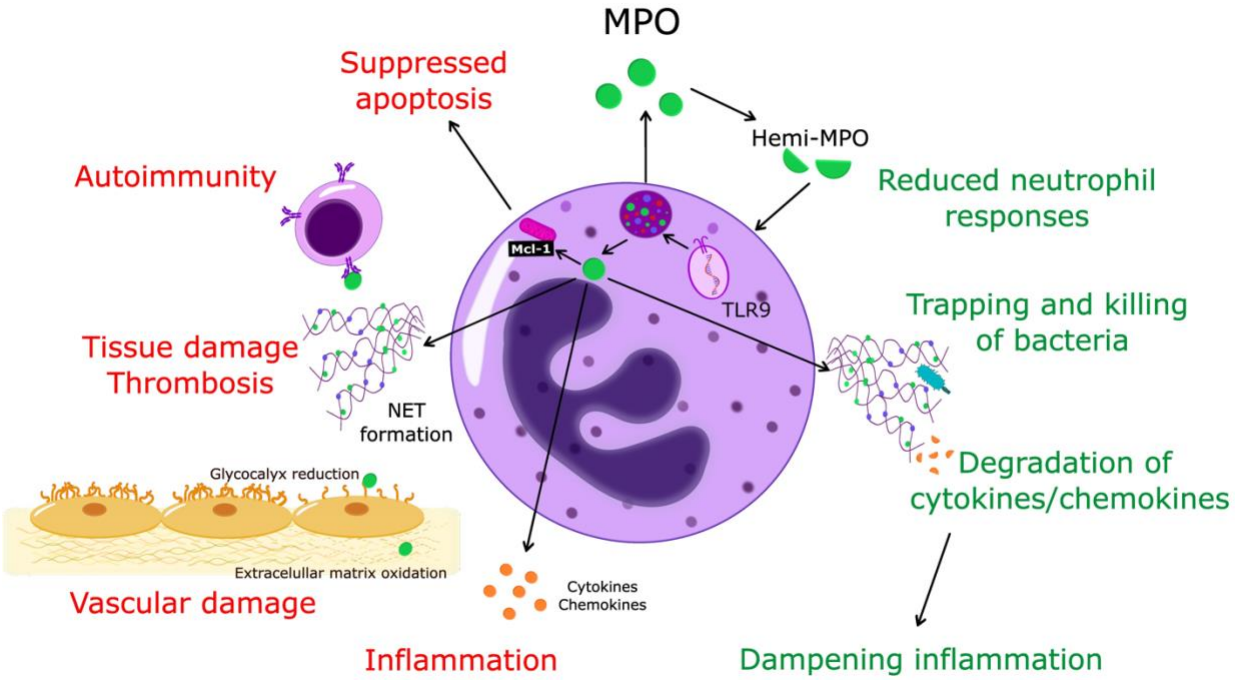

Figure 3. *Dual roles of MPO in inflammation and immune regulation. MPO contributes to both antimicrobial defense (green text) and tissue pathology (red text) [10]*

This neutrophil-centric view of IBD pathogenesis exposes a diagnostic gap. Current tools rely on symptoms, imaging, and histology, which are episodic and indirect. They do not directly index neutrophil effector activity at the mucosal surface, where disease is driven.

2.4 Role of Biomarkers in Diagnosis

Biomarkers that reflect mucosal inflammation are essential for non-invasive monitoring. Three neutrophil-derived proteins are most studied: calprotectin, lactoferrin, and myeloperoxidase. Each has distinct strengths and limitations that determine clinical utility.

2.4.1 Calprotectin

Fecal calprotectin (fCalpro) is the current benchmark non-invasive marker of intestinal inflammation in IBD. Calprotectin is a calcium- and zinc-binding heterodimer of S100A8 and S100A9 abundantly expressed in neutrophils and released into the lumen during active mucosal inflammation. In practice it serves as a surrogate for neutrophil infiltration and helps distinguish IBD from functional disorders such as irritable bowel syndrome (IBS).

Clinical laboratories quantify fCalpro using latex-agglutination turbidimetry or sandwich ELISA platforms [26]. Reported diagnostic performance for differentiating IBD from functional disease is strong, with sensitivities of 80-90% and specificities of 70-85% [24]. A meta-analysis of 2,822 patients found sensitivity 85%, specificity 75%, and AUC 0.88, with higher accuracy in ulcerative colitis than Crohn's disease [27]. Thresholds such as greater than 50 µg/g are commonly used to trigger endoscopic evaluation.

Limitations are biochemical and operational. Calprotectin is susceptible to oxidative modification by HOCl produced by neutrophil MPO, which can alter epitopes and reduce antibody binding in ELISA. Under-recovery is most problematic near decision thresholds and can yield false negatives in low-grade activity. These constraints motivate complementary markers that are less vulnerable to oxidative chemistry and more proximate to neutrophil effector function, such as fMPO.

2.4.2 Lactoferrin / Fecal Calgranulin C (S100A12)

Fecal lactoferrin (fLacto), another neutrophil-derived protein, improves specificity for mucosal ulceration when added to calprotectin testing [28]. In paediatric cohorts, combining fLacto with fecal calgranulin C (S100A12) further enhances diagnostic accuracy for distinguishing IBD from non-inflammatory conditions [29], [30]. The trade-off is practical. Each additional ELISA increases per-test cost, handling steps, and turnaround time, which limits the feasibility of frequent monitoring or decentralised testing.

2.4.3 Fecal Myeloperoxidase

Myeloperoxidase is central to the neutrophil oxidative burst. By converting hydrogen peroxide and chloride into HOCl, fMPO directly reflects active neutrophilic inflammation at the mucosal surface. [22] reported that fMPO discriminated active from quiescent IBD more effectively than fCalpro, with a larger effect size across both CD and UC cohorts. In ulcerative colitis, a study using the UCEIS found stronger correlation of fMPO with endoscopic activity than calprotectin, and higher sensitivity for moderate to severe disease [31].

The barrier to routine use is logistical rather than biological. Most fMPO measurements rely on laboratory ELISA or chemiluminescent assays that require several hours and carry antibody costs, reducing throughput and patient adherence to frequent testing [32]. These constraints justify

development of faster, lower-cost activity-centric methods such as electrochemical sensing that can translate to at-home monitoring.

Table II: Fecal myeloperoxidase (fMPO) concentration cut off ranges [33]

0-49 ug/g	50-199 ug/g	200+ ug/g

Table II discusses the fMPO cut-off ranges that are presented as general bands for both UC and CD, reflecting overlapping distributions of fecal MPO between the two diseases rather than disease-specific thresholds. In UC, values in these bands tend to track more closely with both endoscopic scores and symptom burden, whereas in CD the same concentrations are primarily reflected by mucosal inflammatory activity and are generally less well aligned with patient-reported symptoms, particularly in small bowel predominant disease. The cut-offs should be interpreted as pragmatic ranges of intestinal inflammation across IBD rather than as UC- or CD-specific diagnostic boundaries [33]

2.5 Limitations of Existing Stool-Based Biomarker Assays

Under STRIDE II [19], treatment decisions are time-bound and depend on objective signals. Current stool biomarkers fall short operationally, even when analytically sound.

1. **Slow turnaround and poor adherence**: Standard ELISA workflows typically require over 2 hours to complete, with some protocols taking up to 4.5 hours, making them significantly slower than many blood-based point-of-care tests. This extended processing time can contribute to lower completion rates for fecal ELISA testing compared to more rapid blood-based assays [34]
2. **Under-detection of low-grade inflammation**: Studies suggest oxidation of calprotectin by HOCl can mask mild or subclinical inflammation, leading to false-negative ELISA readings [23].
3. **Cumulative cost and complexity**: Each additional ELISA (e.g., fLacto, S100A12) raises per-test expenses and sample-handling burden [10].

These constraints justify activity-centric, rapid assays that can be deployed outside the laboratory.

2.6 Clinical Relevance and Home-Based Diagnostics

2.6.1 Patient Acceptance and Home-Based Testing

Evidence on patient and clinician acceptance of home fecal testing is mixed and context dependent. The main drivers are turnaround time, perceived accuracy, ease of sampling, and the clarity of action thresholds within a treat-to-target plan [17], [35], [36]

Thomas et al [37] compared four fecal calprotectin assays and showed that platform choice can alter classification around decision thresholds, which undermines clinician confidence that results are interchangeable. That study evaluated analytical agreement but did not address the intrinsic biochemical limitations of calprotectin in oxidising environments or the event-driven nature of neutrophil activity. In practice, delayed or equivocal results miss windows where treatment changes would be most effective.

2.6.2 Development of Comprehensive At-Home Biomarker Kits

An at-home assay that supports STRIDE II [19] should meet four criteria: 1) minimal pre-analytical burden, 2) rapid time-to-result that fits patient routines, 3) resistance to common stool matrix interferences, and 4) outputs that translate directly into care pathways [19].

Multi-marker panels can improve accuracy but add cost and complexity. A pragmatic design is a primary readout that reflects neutrophil effector activity, with a small number of built-in controls that guard against known failure modes. In this context, MPO is attractive because its chemistry reflects the neutrophil oxidative burst at the mucosal surface. A kit that quantifies MPO activity and implements internal checks for oxidative quenching or haem interference can preserve accuracy without recreating lab-grade complexity.

2.7 Diagnostic Innovations

2.7.1 Overview of Non-Invasive Diagnostic Techniques

Non-invasive approaches span breath analysis, stool biomarkers, saliva, urine, point-of-care blood tests, and compact imaging. Their utility depends on three factors: 1) proximity to the mucosal inflammatory process, 2) turnaround time and portability, and 3) robustness to patient-side

variability. Techniques that are distal from neutrophil effector activity or that require laboratory batching are unlikely to support STRIDE II [19] decisions. This chapter evaluates candidate modalities with those constraints in view [38].

2.7.2 Breath-based Diagnostic Methods

Breathomics targets volatile compounds that reflect gut microbial metabolism and host responses. Reported platforms include metal-oxide semiconductor arrays, optical sensors, and hybrid nanocomposites [39]. For example, tungsten trioxide nanoparticles deposited on polyaniline have been used to detect hydrogen at room temperature, enabling simple hardware and rapid readout [39]. These systems are attractive for portability and cost.

However, the limits of breathomics are its specificity to IBD and the depth of its validation in real-world circumstances. Hydrogen elevations also occur in many gastrointestinal conditions and dietary states, and existing studies are small and heterogeneous, so their diagnostic performance for IBS and IBD remains unclear. They also occur in small-intestinal bacterial overgrowth and other dysbioses, so a hydrogen-sensing channel cannot discriminate IBS from these conditions, let alone IBS vs IBD activity [40]. Many studies validate on controlled gas mixtures or small convenience samples, not on prospectively enrolled clinical cohorts with endoscopic ground truth [39]. Diet, recent antibiotics, and inter-individual hydrogen-producer phenotypes also add variance that is hard to control outside a lab setting, and long-term sensor drift and calibration stability remain open issues for home use with this technology [41].

2.7.3 Fecal Sample-Based Volatile Organic Compounds (VOC) Detection

Electronic-nose approaches such as OdoReader attempt to classify stool VOC patterns to infer disease state [42], [43], [44], [45]. Slater et al. [43] evaluated an OdoReader-type platform in children, with stool collected, processed, and analysed by proprietary pattern-recognition algorithms. Reported discrimination suggests signal is present in VOC space, but there are several design constraints that limit translation.

First, VOC signatures are strongly influenced by diet, hydration, recent medications, and timing of collection, which reduces generalisability without strict pre-analytical control [43], [46], [44]. Second, cross-sectional designs cannot link VOC changes to endoscopic improvement or relapse

risk, which is essential for treat-to-target monitoring [43]. Third, the black-box nature of the proprietary algorithms prevents independent assessment of feature stability, overfitting risk, and clinical threshold calibration [43]. Finally, although portable, the current workflow still requires sample preparation, maintenance of sensor heads, and controlled measurement conditions that are not realistic for routine home use [46].

2.7.4 Fecal Calprotectin Methods

Shin et al. [26] benchmarked an automated turbidimetric platform (OC-Sensor Pledia) against a reference ELISA (Phadia 250) and showed comparable diagnostic performance with improved throughput and standardised handling. Automation reduces hands-on time and site-to-site variability and is therefore attractive for routine hospital labs [47].

These gains do not address core timing and proximity problems. Calprotectin assays are not real time; they require extraction, batching, and laboratory processing, which delays decision-making and reduces adherence to frequent testing. The single-analyte dependency is also vulnerable to biochemical and clinical confounders. Oxidative modification can alter epitopes and depress recovery near decision thresholds, while non-IBD inflammation, infections, and medications can elevate values and create diagnostic ambiguity [27], [48]. In short, calprotectin platforms are better laboratory tools than home tools and remain indirect readouts of neutrophil activity.

Because clinical studies still support faecal calprotectin as the most widely validated stool marker of neutrophil-driven inflammation, there has been a push to adapt it into portable, near-patient formats. IBDoc represents this shift: a home-use calprotectin platform developed to deliver quantitative FC results outside the laboratory.

IBDoc is a CE-IVD (certified in-vitro diagnostic) home faecal calprotectin test that couples a lateral flow cassette with a dedicated stool extraction device (CALEX Valve) and a smartphone application, allowing patients to generate quantitative fecal calprotectin results remotely in their own homes. The app converts the phone camera into a reader for the test strip and uploads data to a clinician portal, enabling telemonitoring and tighter treat-to-target management without requiring hospital visits or central laboratory access [20]. Clinical evaluations in adult and paediatric IBD cohorts have shown good agreement between IBDoc and laboratory-based methods (ELISA and Quantum Blue), with correlation coefficients around 0.8–0.9 and high concordance

in the low moderate fecal calprotectin range, alongside high patient acceptability and willingness to use the test for ongoing monitoring. These studies support IBDoc as a feasible tool for remote fecal calprotectin based disease tracking and e-health programmes [49], [50].

However, IBDoc inherits the core biochemical and interpretive limitations of calprotectin itself. It remains a single-analyte protein assay that reports an indirect surrogate of neutrophil activity and is still susceptible to signal distortion by non-IBD inflammation, infections, medications and pre-analytical factors. Analytical agreement with ELISA is strongest below ~500 µg/g, with reduced reliability at higher concentrations where confirmation by a laboratory method is recommended, and performance depends on correct sampling, smartphone compatibility and user technique [51].

Thus, while IBDoc improves proximity and convenience compared with conventional lab-based fecal calprotectin testing, it does not resolve the underlying limitations of calprotectin as an indirect, protein-mass readout of intestinal inflammation, reinforcing the case for complementary, activity-based biomarkers such as MPO.

2.7.5 Fluorescence-Based Detection of IBD Biomarkers

Fluorescence immunoassays and microfluidic fluorescence devices offer high analytical sensitivity and potential multiplexing. In practice, translation to at-home testing is constrained by matrix autofluorescence, haem and bile pigment quenching, photobleaching, optical alignment tolerance, and the need for dark-box optics. Incubation steps and wash cycles extend time-to-result and add user error [52], [53]. Fluorescence is therefore best positioned for near-patient labs rather than unsupervised home monitoring.

By taking advantage of MPO, a frontline neutrophil enzyme, through a rapid fluorescence reaction can capture real-time oxidative activity. Unlike passive biomarker accumulation measured over hours or days, MPOLR delivers a mechanistically anchored snapshot within minutes, shifting the diagnostic paradigm from proxy inference to functional immediacy.

Myeloperoxidase-Luminol Reaction (MPOLR) is a five-minute chemiluminescent assay for fecal MPO, eliminating antibodies and lengthy incubations [14]. In 45 IBD patients and 19 controls, peak luminol emission (captured on a multimode reader) correlated strongly with ELISA-derived fMPO ($\rho = 0.82$) and, in ulcerative colitis, outperformed fecal calprotectin for endoscopic score (ρ

= 0.78 vs 0.58) and symptom index (ρ = 0.78 vs 0.41). The optical signal relies on rapid HOCl-mediated luminol oxidation and thus demands precise timing and laboratory imaging hardware, while blood or non-MPO peroxidases can confound quantification, which is reported in relative light units rather than absolute concentration [1], [54].

Fig. 4 summarises the recruitment pipeline and laboratory workflow used in MPOLR. Stool samples were collected from all participants. For patients with ulcerative colitis (UC) and colonoscopy controls (CC), samples were taken just before bowel preparation. UC disease activity was assessed using the UCEIS scoring system, while CC patients showed no visible inflammation during colonoscopy and had no history or future diagnosis of IBD. Healthy controls (HC) did not undergo colonoscopy.

To reduce variability within each sample, a three-point sampling method was used before combining the material. Samples were then treated with DNase, briefly spun down (1,000 rpm for 30 seconds), and diluted to 5% weight/volume.

Three biomarkers: fMPO, fCalpro, and fLacto were quantified using ELISA assays. MPO enzyme activity was also measured using a custom setup involving MPOLR reaction buffer and a Raspberry Pi-powered detection device. Finally, pairwise statistical comparisons were made between clinical scores and each biomarker level.

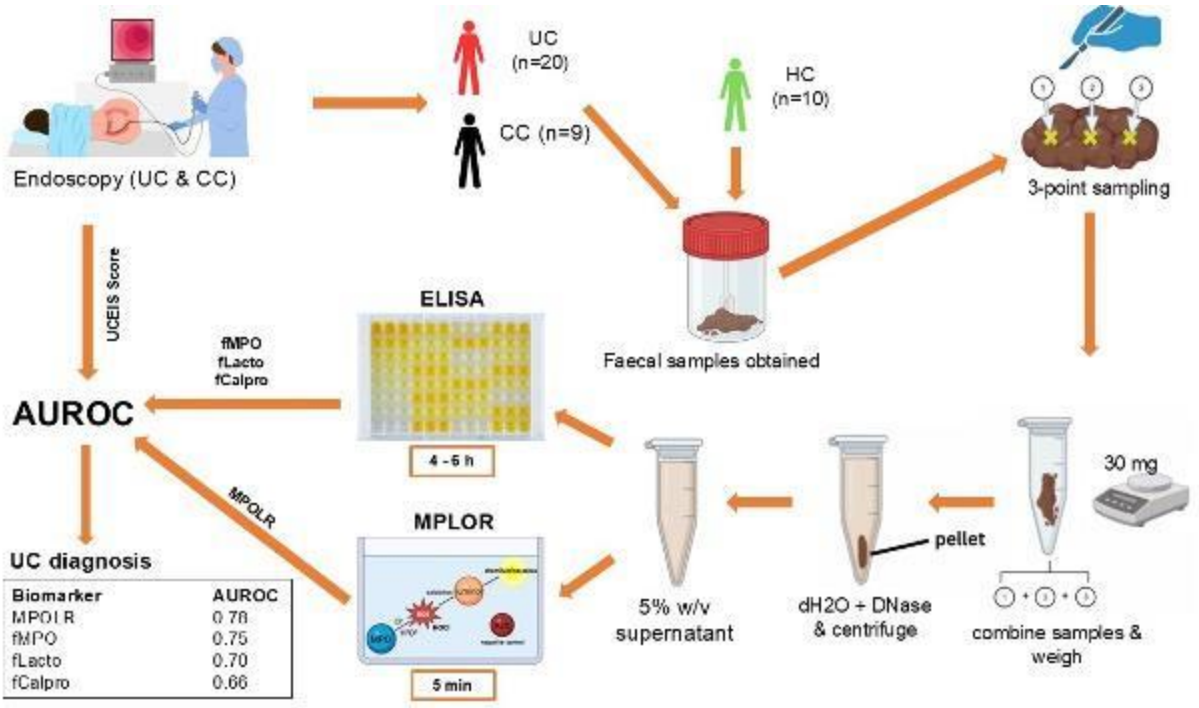

Figure 4. *Visual abstract of the clinical study design and fecal-sample processing pipeline used for MPOLR validation [1]*

Although this method represents a novel diagnostic approach, Kariyawasam et al. [1] acknowledges several technological limitations that currently constrain its translational potential. MPOLR lacks biochemical specificity, as it detects chemiluminescence from any peroxidase capable of oxidising luminol (such as eosinophil peroxidase, horseradish peroxidase, or haemoglobin), rather than MPO alone, increasing the risk of off-target signal. This is compounded by a high false-positive potential in the presence of occult blood, which is common in IBD and other gastrointestinal conditions: haemoglobin can drive luminol oxidation via Fenton-type reactions, generating light emission unrelated to MPO-derived HOCl. Inhibitor controls were also incomplete, with the MPO inhibitor AZD3241 failing to fully suppress luminescence, suggesting partial MPO inhibition and/or alternative luminol oxidation pathways, and thereby raising further concerns about assay fidelity. At the hardware level, luminol's rapid post-oxidation decay creates a narrow detection window that demands tightly synchronised reagent injection and signal capture; although Chemidoc imaging enabled whole-plate readout, it lacks integrated injection control and real-time kinetic resolution. Finally, MPOLR outputs signal in relative light units rather than calibrated concentration, limiting clinical interpretability and preventing direct alignment with

standardised diagnostic thresholds used in practice. Despite these constraints, the study validates the core strength of MPO-centred chemistry: its capacity to deliver rapid, proximal insight into neutrophil-driven inflammation using inexpensive reagents. These properties make it a strong candidate for translation into calibrated electrochemical detection systems, a future direction explicitly suggested by [1] for enabling decentralised, real-time diagnostics.

Despite these constraints, the study validates the core strength of MPO-centred chemistry: its capacity to deliver rapid, proximal insight into neutrophil-driven inflammation using inexpensive reagents. These properties make it a strong candidate for translation into calibrated electrochemical detection systems, a future direction explicitly suggested by Kariyawasam et al. [1] for enabling decentralised, real-time diagnostics.

2.8 Transition to Electrochemical Detection Methods

Taken together, these limitations in luminol-based MPOLR and other studies motivate a shift towards electrochemical transduction of MPO activity. Electrochemical methods directly monitor redox transformations at an electrode surface, can be calibrated in absolute concentration units, and are inherently compatible with disposable screen-printed electrodes and portable potentiostats. By tuning the redox probe chemistry and electrode interface, they also offer greater scope to preferentially capture MPO-derived oxidants while minimising interference from haemoglobin and other peroxidases. The following section therefore examines electrochemical detection strategies, beginning with serum-based assays, to identify design principles that can be adapted for faecal, point-of-care IBD diagnostics.

2.8.1 Electrochemical Detection in Serum Samples

Recent advances in label-free voltammetry demonstrate the viability of these systems. For example, Sciurti et al. [55] designed a label-free voltammetric sensor for Oncostatin M (OSM), an inflammation-associated cytokine, by immobilising a mixed self-assembled monolayer on gold and monitoring charge-transfer resistance changes after protein binding [18]. In human-serum trials the device achieved sub-nanomolar limits of detection without antibodies or enzymatic labels, demonstrating that carefully engineered electrode surfaces can yield quantitative readouts with minimal sample preparation. However, Sciurti et al. [1] was confined to a relatively clean matrix and noted that high particulate loads, proteases and variable ionic strength in stool would

require additional anti-fouling layers or pre-treatment steps. So, while the work does validate label-free electrochemistry for protein biomarkers, its direct translation to complex fecal analysis is unknown.

2.8.2 Advancements in Electrochemical Detection of MPO

Label-free voltammetry can detect protein biomarkers reliably in controlled solutions, but fecal samples are much harsher: enzymatic degradation, solid particulates, and electroactive contaminants all distort the signal unless the electrochemical design is robust to matrix effects. Recent work has begun to target MPO electrochemically, mainly via mediator-based signal amplification in solution or surface-engineered electrodes that resist fouling and improve selectivity. These studies [56], [57] confirm that MPO's peroxidase activity can be converted into a quantifiable electrochemical read-out, but they also highlight the main obstacle to stool applications: matrix interference, rather than lack of intrinsic sensitivity. Table III summarises two representative strategies and illustrates how well they perform in clean media versus why they are likely to struggle in fecal deployment.

Table III. Electrochemical strategies for MPO quantification: mediator-based versus surface-engineered approaches

Study	Principal Strategy	Strengths	Matrix-related limitations
Hoyo et al. [56]	Ferrocene-based redox mediator that reports MPO-generated hypochlorous acid via amperometric read-out.	Rapid, reagent-minimal signal generation in simple buffer, demonstrating effective transduction of MPO activity.	Vulnerable to competing oxidants and fouling. Stool-compatible sample preparation or mediator protection have also not been demonstrated.
Nandeshwar & Tallur [57]	Diazonium-modified ENIG PCB electrodes that detect MPO through catalytic reduction of hydrogen peroxide.	Low-cost PCB platform with a surface film that improves selectivity over bare gold in biofluids.	Evaluated only in plasma. Faecal particulates and enzymes are likely to destabilise the film and distort baseline currents, thus requiring more robust or disposable electrodes.

Whilst the studies in Table III do confirm that MPO's peroxidative chemistry can be transduced electrochemically, they highlight the biochemical complexity of feces especially solids, mucins, and microbial oxidants which are the main technical obstacles.

2.8.3 Next-Generation Electrochemical Sensors

To overcome these limitations, recent innovations have focused on nanomaterial-based sensors that combine sensitivity, miniaturisation, and disposability. Two emerging approaches stand out: quantum-dot-based immunosensors and graphene screen-printed electrodes [58], [59]. These systems demonstrate how electrode architecture, surface functionalisation, and fabrication method can be tuned for specific use cases for point-of-care devices, high sensitivity versus low-cost scalability. Table IV compares these platforms and outlines their potential adaptability for fecal MPO detection.

Table IV. Next-generation electrochemical MPO sensors: quantum-dot ultra-sensitive versus graphene low-cost platforms

Sensor concept	Technical advance	Reported performance	Considerations for fecal MPO
Yanbing et al. [58] - quantum dot immunosensor	Uses a quantum-dot enhanced electrode with a sandwich-style antibody assay to boost the electrical signal from MPO.	Extremely sensitive - able to detect very small amounts of MPO and cover both low and high disease activity in one test.	Reliance on antibodies and complex nanomaterials, increasing burden on cost and usually requiring a cold chain. Cleaning and re-use of chip is unrealistic, making it harder to adapt into cheap, single use stool cartridges
Valdivieso et al. [59] - screen-printed carbon immunosensor (saliva MPO)	Uses disposable printed carbon strips coated with antibodies for MPO, designed for simple, low-cost measurements.	Gives clear discrimination between low and high MPO and matches well with standard laboratory methods in saliva.	Stool particulates and proteases could foul the carbon surface; the 2 - 4 h drying step and need for supernatant clarification is too slow and complicated for point of care fecal testing.

Both quantum-dot-based immunosensors and graphene screen-printed electrodes present promising advances in point-of-care electrochemical sensing, yet each solution suffers from technological limitations that affect their suitability for fecal MPO detection. Quantum-dot platforms, such as the CdSe/ZnS-based device developed by Yanbing. et al. [58] rely on complex fabrication involving nanocrystal synthesis and antibody immobilisation, necessitate cold-chain storage, and are impractical for single-use applications due to their cost and lack of regenerability.

Their amperometric signals can also suffer from photo-instability and integration challenges with portable readers [60], [61], [62]

In contrast, the graphene screen-printed strips developed by Valdivieso et al. [59] can be mass-produced cheaply and deliver amperometric readings within seconds; however, their unprotected carbon–graphene surfaces are rapidly fouled by stool particulates and enzymes, so anti-fouling coatings and built-in filtration pads are required to maintain reliable signal fidelity.

These constraints highlight a gap in the field for a sensor platform that is both oxidation-specific and engineered for matrix tolerance, without dependence on biological capture elements or fragile nanomaterials.

2.8.4 The Proposed Solution: Printed Electrochemical MPO Sensor (PIEMS)

To address the limitations of current assays and narrow the gap between laboratory-grade precision and point-of-care use, the Printed Electrochemical MPO Sensor (PIEMS) is proposed: an SPE-based platform that reports MPO activity via its oxidant products rather than antibody binding. Instead of capturing MPO with immobilised antibodies, PIEMS detects MPO-derived HOCl and related oxidants through their effect on a ferrocyanide/ferricyanide redox couple at a disposable SPE working electrode. Under controlled oxidant conditions (HOCl, H_2O_2), changes in voltammetric peak currents provide a monotonic, calibratable relationship between signal and oxidant concentration, which can be back-translated to MPO activity in fecal extracts. Because the readout is based on catalytic function rather than epitope integrity, the platform is less vulnerable to oxidative and proteolytic damage that can compromise antibody-based ELISAs in highly inflamed stool. The SPE format is inherently low-cost, single-use, and compatible with compact potentiostats such as the Palmsens family, and the chemistry requires only simple aqueous reagents, making the architecture well suited to miniaturisation and integration into an at-home workflow for fast, quantitative, fecal-based IBD monitoring.

In the present work, cyclic voltammetry is used to establish and optimise this sensing chemistry: CV characterises the ferrocyanide/ferricyanide couple, defines an appropriate potential window, and quantifies how increasing HOCl/TauCl suppresses the anodic peak current. This provides a robust mechanistic and analytical foundation but remains relatively time-consuming and less sensitive than pulse techniques. Future development of PIEMS for true point-of-care deployment

should therefore transition to differential pulse voltammetry (DPV), which offers improved background suppression, higher sensitivity and shorter measurement times, and is better aligned with low-power, handheld potentiostat platforms such as PalmSens [63].

The proposed workflow is informed by existing home-use faecal calprotectin platforms such as IBDoc, which demonstrate that stool collection, cartridge-based extraction and smartphone-mediated result delivery are feasible and acceptable in routine care. The conceptual PIEMS system mirrors this overall architecture, a standardised stool sampling device, a sealed single-use cartridge and a compact reader or phone-linked potentiostat [63] while substituting calprotectin protein-mass measurement with MPO activity-based electrochemistry as the underlying signal.

Chapter 3: Methodology

3.1 Reagents, Materials and Instrumentation

Materials related to electrochemical instrumentation, including a computer-controlled potentiostat (ZIVE), screen-printed carbon electrodes (DropSens, Spain), a glass-body Ag/AgCl reference electrode and a glassy carbon counter electrode, were obtained from commercial electrochemistry suppliers via the University of Sydney MyLab ordering system.

Materials related to the PIEMS reaction were sourced from Sigma-Aldrich (Merck), including 9.7 M hydrogen peroxide (Cat. No. 386790), 0.277 M sodium hypochlorite (Cat. No. 425044), sodium chloride (Cat. No. S5886), taurine (Cat. No. 8086160005), potassium ferrocyanide trihydrate ($K_4[Fe(CN)_6]\cdot 3H_2O$) and phosphate-buffered saline (PBS) tablets. The MPO inhibitor AZD3241 (PXS-5398) was sourced from Pharmaxis, Frenchs Forest, Sydney, Australia. Samples of myeloperoxidase (MPO) were provided as sterile biochemical preparations by the Charles Perkins Centres at the University of Sydney.

3.2 Overview of experimental strategy

This methodology quantifies HOCl via its effect on the ferrocyanide/ferricyanide redox couple and then translates that chemical readout into an estimate of MPO activity. The strategy is deliberately split into two linked experimental arms. First, a chemically defined calibration is established in which known doses of HOCl, stabilised as taurine chloramine (TauCl), are titrated into a ferrocyanide solution and the resulting changes in the ferricyanide anodic peak current are measured under oxygen-free conditions. This provides a controlled relationship between oxidant concentration and CV signal and defines the linear range, sensitivity, and repeatability of the electrode–electrolyte system.

In the second arm, this calibration is applied to a biologically relevant MPO system. Here, HOCl is generated *in situ* from MPO, hydrogen peroxide (H_2O_2), and chloride on small-volume droplets placed on screen-printed carbon electrodes. The same ferrocyanide/ferricyanide couple is used as the electrochemical reporter, and optional inclusion of the MPO inhibitor AZD3241 and the protective protein bovine serum albumin (BSA) allows the impact of pharmacological inhibition and protein-rich environments on the oxidant signal to be assessed. By mapping the MPO-driven suppression of the ferrocyanide peak onto the previously derived TauCl calibration, the combined

approach converts CV peak changes into quantitative estimates of MPO-derived oxidant, providing a coherent framework for fMPO assay development.

3.3 Chemical Calibration of HOCl/TauCl using Ferrocyanide Voltammetry

This phase of the work established a quantitative relationship between oxidant dose and electrochemical signal by titrating taurine chloramine (TauCl) into a ferrocyanide solution and measuring the resulting changes in the ferricyanide oxidation current. The calibration obtained here is later used to translate voltammetric signals into an estimate of MPO activity.

3.3.1 Preparation of HOCl and TauCl Solutions

HOCl was supplied as a certified laboratory bleach solution. Its active chlorine concentration was standardised spectrophotometrically to obtain an HOCl molarity of 9.27 mM. Taurine was dissolved in 10 mM phosphate-buffered saline (PBS) to prepare a 9.27 mM taurine solution, thus matching the HOCl concentration and enabling a 1:1 stoichiometric reaction.

TauCl was generated immediately prior to calibration experiments by mixing the 9.27 mM HOCl and 9.27 mM taurine solutions in a 1:1 ratio (v/v) in 10 mM PBS. This ensured that free HOCl was rapidly converted into the more stable chloramine species (TauCl), reducing problems associated with HOCl instability, decomposition, and uncontrolled side reactions. All solutions in this phase, including ferrocyanide and any dilutions, were prepared in 10 mM PBS to maintain a consistent ionic environment.

3.3.2 Ferrocyanide Electrolyte and TauCl Titration

The reporting redox couple was ferrocyanide/ferricyanide. A 500 µM solution of potassium ferrocyanide ($K_4[Fe(CN)_6]$) was prepared in 10 mM PBS and used as the base electrolyte after a range of concentrations (50 µM, 500 µM, and 5 mM) was tested to identify the optimal condition (see appendix 1). Calibration was performed by stepwise addition of TauCl into this ferrocyanide solution to achieve final TauCl concentrations spanning 0 - 280 µM.

At each titration step, a defined volume of the TauCl stock was added to the ferrocyanide solution, and the bulk solution was homogenised to pre-distribute the oxidant. Three independent titration series (n = 3) were performed to assess reproducibility across runs.

3.3.3 Electrochemical cell configuration

Electrochemical measurements were carried out in a three-electrode configuration:

- **Working electrode (WE):** SPE working electrode
- **Reference electrode (RE):** Ag/AgCl reference electrode
- **Counter electrode (CE):** glassy carbon electrode

The ferrocyanide/TauCl solution was placed in an electrochemical cell such that the SPE working electrode, Ag/AgCl reference, and glassy carbon counter were all immersed in the same electrolyte volume. This arrangement enabled controlled, reproducible measurements of the ferrocyanide/ferricyanide redox response under defined oxidant conditions.

3.3.4 Oxygen Removal and Solution Homogeneity

Preliminary experiments demonstrated that dissolved oxygen produced significant background currents and overlapping peaks within the potential window relevant for ferrocyanide and HOCl/TauCl, degrading peak resolution and quantitative accuracy. To minimise oxygen interference, the electrolyte in the cell was purged with nitrogen gas (N_2) prior to the trial. This deoxygenation step was critical to suppress oxygen reduction currents and stabilise the baseline.

Solution homogeneity was also identified as a key determinant of signal quality. Initial trials without active mixing showed visible layering in the cell and inconsistent peak currents, consistent with concentration gradients of TauCl or ferrocyanide near the electrode. To address this, the solution was thoroughly mixed (via magnetic stirring) between additions to ensure uniform distribution of TauCl throughout the electrolyte. Stirring was stopped just before each voltammetric scan to re-establish a quiescent diffusion layer at the working electrode. This was particularly important at the relatively low ferrocyanide concentration (500 µM), where small local concentration differences can disproportionately affect current response.

Figure 5. *Visible layering of ferrocyanide*

3.3.5 Cyclic Voltammetry Protocol

Cyclic voltammetry (CV) was used to interrogate the ferrocyanide/ferricyanide redox couple in the presence of increasing TauCl concentrations. The potential was swept from –0.50 V to +0.80 V versus Ag/AgCl at a scan rate of 20 mV/s, with a potential step (sampling interval) of 5 mV. Each experiment consisted of six segments corresponding to multiple consecutive cycles. Before the first scan, the system was allowed to equilibrate by applying an initial delay of 1 min 40 s at open circuit, followed by a 2 s quiet time at the initial potential. The current range on the potentiostat was set to 1 A with auto-ranging enabled and a 1 A compliance limit to avoid signal clipping at higher currents, and no deposition (pre-concentration) step or iR compensation was applied. For each TauCl concentration, three consecutive CV cycles were recorded; the third cycle was used for analysis to allow transient charging currents to decay and for the electrode surface and double layer to re-equilibrate under the new solution conditions.

3.3.6 Peak extraction and calibration curve construction

For each CV, the anodic peak corresponding to the oxidation of ferrocyanide to ferricyanide ($Fe(CN)_6^{4-} \rightarrow Fe(CN)_6^{3-}$) was identified on the forward scan of the third cycle. Code was developed to streamline but failed consistently to map the peaks reliably and so current–potential data were exported to OriginPro for manual processing (See appendix 2). A manual baseline around the oxidation peak region was defined and subtracted to isolate the faradaic peak current from the capacitive background.

Peak anodic currents were then plotted as a function of TauCl concentration (or cumulative TauCl volume added) to construct the calibration curve.

Across three independent titration runs, this approach allowed assessment of the linearity of the current–concentration relationship, the sensitivity of the assay (slope of the calibration), and the between-run variability and repeatability. The resulting calibration, established under oxygen-free conditions in a well-defined TauCl/ferrocyanide system, provides the quantitative link between oxidant concentration and electrochemical signal. In later stages, this relationship could be used to back-calculate MPO activity from electrochemical data obtained in more complex matrices (e.g. spiked or clinical stool extracts), where HOCl generated by MPO is effectively "captured" as TauCl and read out via the same ferrocyanide/ferricyanide redox couple.

3.4 Enzymatic MPO assay: In situ HOCl generation on Screen-printed Carbon Electrodes

The second arm of the methodology used an enzymatic MPO system to generate HOCl in situ from MPO, H_2O_2 and chloride and to read out this activity via the ferrocyanide/ferricyanide redox couple on SPEs. This experiment translated the ferrocyanide–TauCl calibration into a biologically relevant MPO–H_2O_2–Cl^- context and assessed the impact of pharmacological inhibition (AZD3241) and protein protection (BSA) on the electrochemical signal.

3.4.1 Reagents and Stock Solutions

All reagents were prepared in 10 mM PBS, consistent with the chemical calibration arm.
The following stock solutions were used:

- Ferrocyanide: 500 µM $K_4[Fe(CN)_6]$ stock in 10 mM PBS, diluted to the same working ferrocyanide concentration used in the TauCl calibration.
- NaCl: 200 mM NaCl in PBS as the chloride source for MPO.
- H_2O_2: 20 mM hydrogen peroxide in PBS, freshly prepared and kept cold and protected from light.
- Taurine: Prepared in 10 mM PBS at a concentration chosen to give an approximate 1:1 molar ratio with H_2O_2-derived HOCl, mirroring the earlier TauCl strategy so that HOCl formed by MPO was rapidly captured as TauCl.
- MPO: Myeloperoxidase working solution at 1 µg/mL in 10 mM PBS.

Inhibitor and protective protein:

- AZD3241 (MPO inhibitor): 180 µM stock was prepared. 10 µL of this stock was added into each 70.4 µL reaction.

- BSA: A 1 mg/mL BSA working solution was prepared and when required, 5 µL was added per 70.4 µL reaction.

All components were diluted with 10 mM PBS to achieve the desired working concentrations while keeping total volume per measurement fixed at 70.4 µL.

3.4.2 Droplet-based Reaction Assembly on SPEs

Electrochemical measurements were performed using disposable SPEs with integrated working, reference, and counter electrodes on a single substrate. No external reference or counter electrodes were used; all reactions were confined to a single 70.4 µL droplet dispensed directly onto the SPE.

For each run:

1. A reaction mixture containing MPO, NaCl and ferrocyanide (and, when appropriate, AZD3241 and/or BSA) was assembled in a microtube and briefly vortexed to ensure mixing.
2. An aliquot was pipetted onto the SPE such that the total droplet volume was 70.4 µL, just sufficient to cover the printed working, reference and counter tracks.
3. Immediately before starting the voltammetric scan, H_2O_2 and taurine were pipetted directly into this droplet on the SPE surface to initiate the MPO reaction (MPO + H_2O_2 + Cl^- → HOCl, rapidly converted to TauCl in the presence of taurine).
4. Cyclic voltammetry was started immediately after H_2O_2/taurine addition to capture the oxidant-driven modulation of the ferrocyanide/ferricyanide signal under well-defined reaction conditions.

This droplet-based format minimised reagent consumption and justified the use of the SPE as a self-contained three-electrode system.

3.4.3 Experimental conditions

Two main conditions were examined, each performed in triplicate (n = 3). In the MPO + inhibitor condition, the droplet contained MPO, NaCl, ferrocyanide, and the small-molecule inhibitor

AZD3241, and was used to assess how direct MPO inhibition affects oxidant generation and the resulting suppression of the ferrocyanide peak. In the MPO + inhibitor + BSA condition, MPO, NaCl, ferrocyanide, AZD3241, and BSA were combined to investigate whether a more protein-rich environment, through oxidant scavenging, surface protection, or broader matrix effects, alters MPO-driven oxidant output or the electrochemical readout. In all cases, H_2O_2 and taurine were added last on the SPE droplet to initiate HOCl/TauCl formation under otherwise identical conditions.

3.4.4 Voltammograms and Link to calibration

Cyclic voltammetry was performed using the same acquisition parameters and data-processing approach as in the TauCl ferrocyanide calibration arm established in 3.3, to preserve comparability.

For each trial, the anodic ferrocyanide-to-ferricyanide peak current from the analysed cycle was extracted and mapped onto the previously established ferrocyanide - TauCl calibration curve. This mapping converted peak suppression in the enzymatic assays into an "equivalent" TauCl/HOCl concentration, enabling quantitative estimation of MPO-derived oxidant under each condition (± AZD3241, ± BSA) and allowing direct comparison of enzymatic MPO behaviour with the chemically controlled TauCl system. In this way, the enzymatic assay uses the first arm's calibration as its interpretive backbone, turning changes in CV peak current from small-volume droplets on SPEs into quantitative estimates of MPO activity.

In this way, the enzymatic assay uses the first arm's calibration as its interpretive backbone, turning changes in CV peak current from small-volume droplets on SPEs into quantitative estimates of MPO activity.

Chapter 4 – Results

The purpose of this chapter is to present the findings that informed the development of an at-home diagnostic concept for IBD. The chapter begins with the chemical calibration and electrochemical analysis of hypochlorous acid (HOCl) and taurine chloramine (TauCl), selected as key biomarkers due to their role in neutrophil-mediated inflammation. This is followed by an evaluation of the analytical performance of these compounds using screen-printed electrodes, including signal characteristics and buffer compatibility. Finally, the chapter introduces a conceptual device design that integrates these experimental insights into a multi-chamber system with safety features and a portable potentiometric interface

4.1 HOCl/TauCl Chemical Calibration

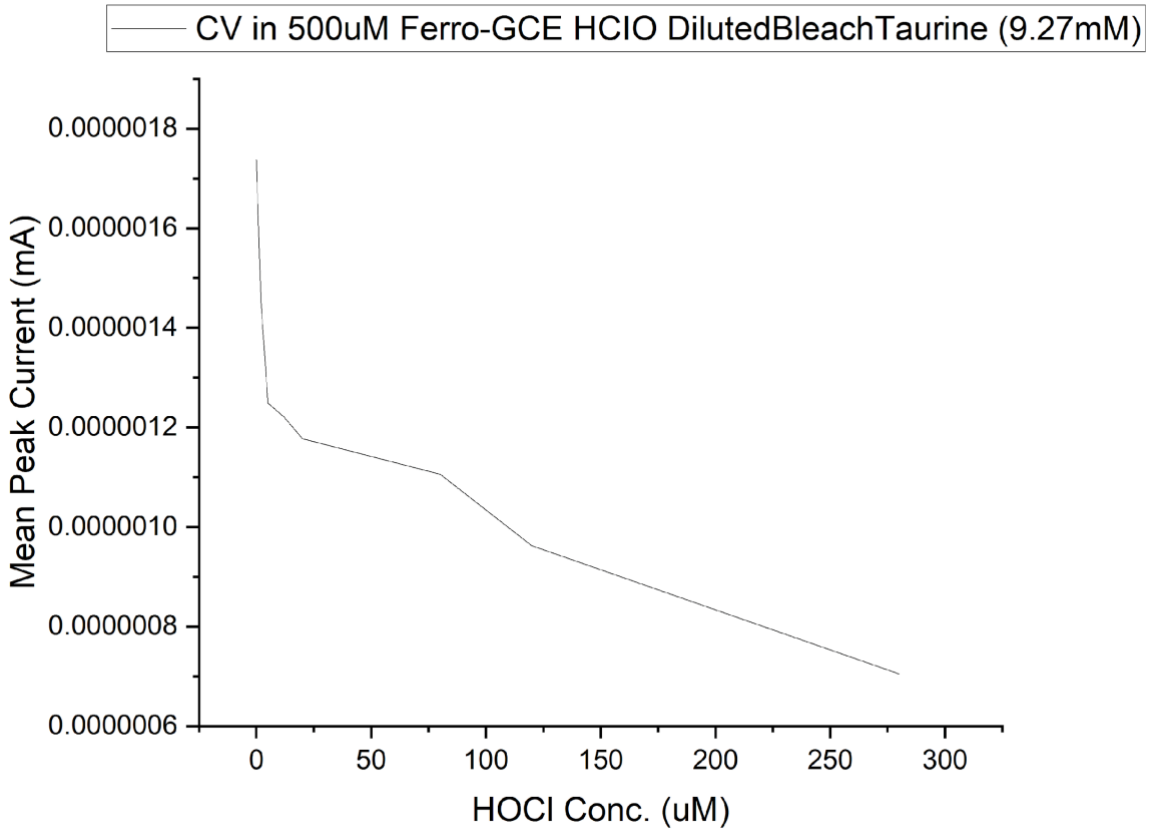

***Figure 6**. TauCl Concentration influence on Ferrocyanide*

4.1.1 Dose–response behaviour

Fig. 6 shows the effect of increasing oxidant dose on the ferrocyanide oxidation peak. In 500µM ferrocyanide, the anodic peak current was highest in the absence of HOCl/TauCl and fell sharply upon the first low-micromolar additions of oxidant. Beyond this initial drop, the peak current

decreased approximately linearly as the HOCl/TauCl concentration increased up to ~300µM, yielding a clear monotonic dose–response relationship that can be used to back-calculate oxidant concentration from current.

4.1.2 Analytical sensitivity, LOD and LOQ

Because HOCl was mixed 1:1 with taurine, the x-axis effectively represents the concentration of TauCl formed from HOCl. When the current changes measured in the enzymatic MPO experiments were mapped onto this chemical calibration curve, the smallest MPO-driven signal that could be distinguished from the blank corresponded to 2.4 µM TauCl, and reliable quantification was achieved from 7.9 µM TauCl. Thus, at an MPO concentration of 1 µg/mL, the assay provided an estimated limit of detection (LOD) of 2.4 µM TauCl and a limit of quantification (LOQ) of 7.9 µM TauCl, expressed as equivalent TauCl concentration.

4.2 Miniaturisation Roadmap and Device Concept

The miniaturisation roadmap outlines how the current bench-top assay can be translated into a deployable diagnostic device, progressing from the current bench-top workflow kit to an in-home test. In this context, the workflow is the ordered sequence of sample-processing and measurement steps that convert a stool specimen into a quantitative MPO result, and it provides the template for subsequent cartridge and instrument design.

4.2.1 Bench-top Electrochemical Workflow

In parallel with assay development, a roadmap was drafted for how the current bench-top workflow could be translated first into a pathology-lab kit and ultimately into an in-home test *(Fig. 7,8,9,11)*. In the current laboratory implementation, stool is collected at home and delivered to pathology, where fMPO is extracted using a standard ELISA-style preprocessing pipeline. For the electrochemical assay, known concentrations of MPO are combined with a "test solution" containing NaCl, AZD3241, BSA and ferrocyanide. This mixture is pipetted onto the working electrode, followed by a defined volume of an "activation solution" containing H_2O_2 and taurine. Cyclic voltammetry is then run immediately, and the peak current is compared with the chemically generated TauCl calibration curve to back-calculate the equivalent TauCl concentration and, by extension, MPO activity. This defines the minimal set of liquid-handling steps that any miniaturised device must reproduce: MPO extraction, mixing with the test solution, activation with H_2O_2/taurine and real-time current read-out.

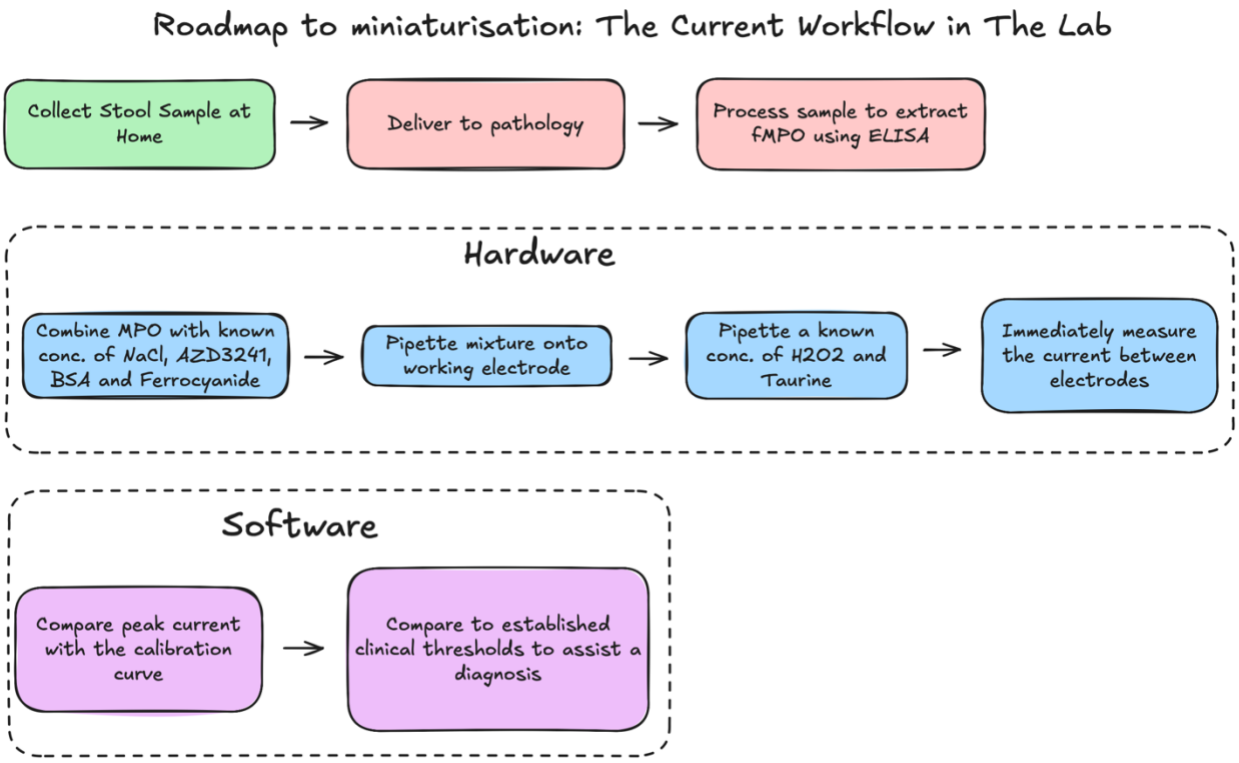

***Figure** 7. Current Laboratory Workflow*

4.2.2 Pathology-kit Workflow

Building on the bench-top protocol, an intermediate pathology-kit workflow is proposed as shown by *Fig 8*. In this scenario, stool collection and fMPO extraction remain centralised in a pathology laboratory, but the read-out is performed using a dedicated electrochemical kit rather than a research potentiostat. This intermediate step is intended to improve analytical consistency and turn-around time while providing a STRIDE II [19] aligned bridge between a fully manual research assay and a future patient-operated test. The test and activation solutions are pre-made, premixed and refrigerated in labelled vials. After extraction, the pathology scientist combines the fMPO sample with the test solution, uses a disposable dropper to deposit the mixture onto a screen-printed working electrode, and then adds the activation solution using a second dropper. A portable handheld potentiostat such as those mentioned in [64], [65] performs the CV scan on the disposable sensor. Embedded software compares the measured peak current with the stored calibration curve and returns an MPO concentration that can be mapped directly onto clinical fMPO ranges to assist diagnosis. This step preserves existing laboratory logistics while de-risking the assay chemistry in a format that is already close to a commercial pathology product.

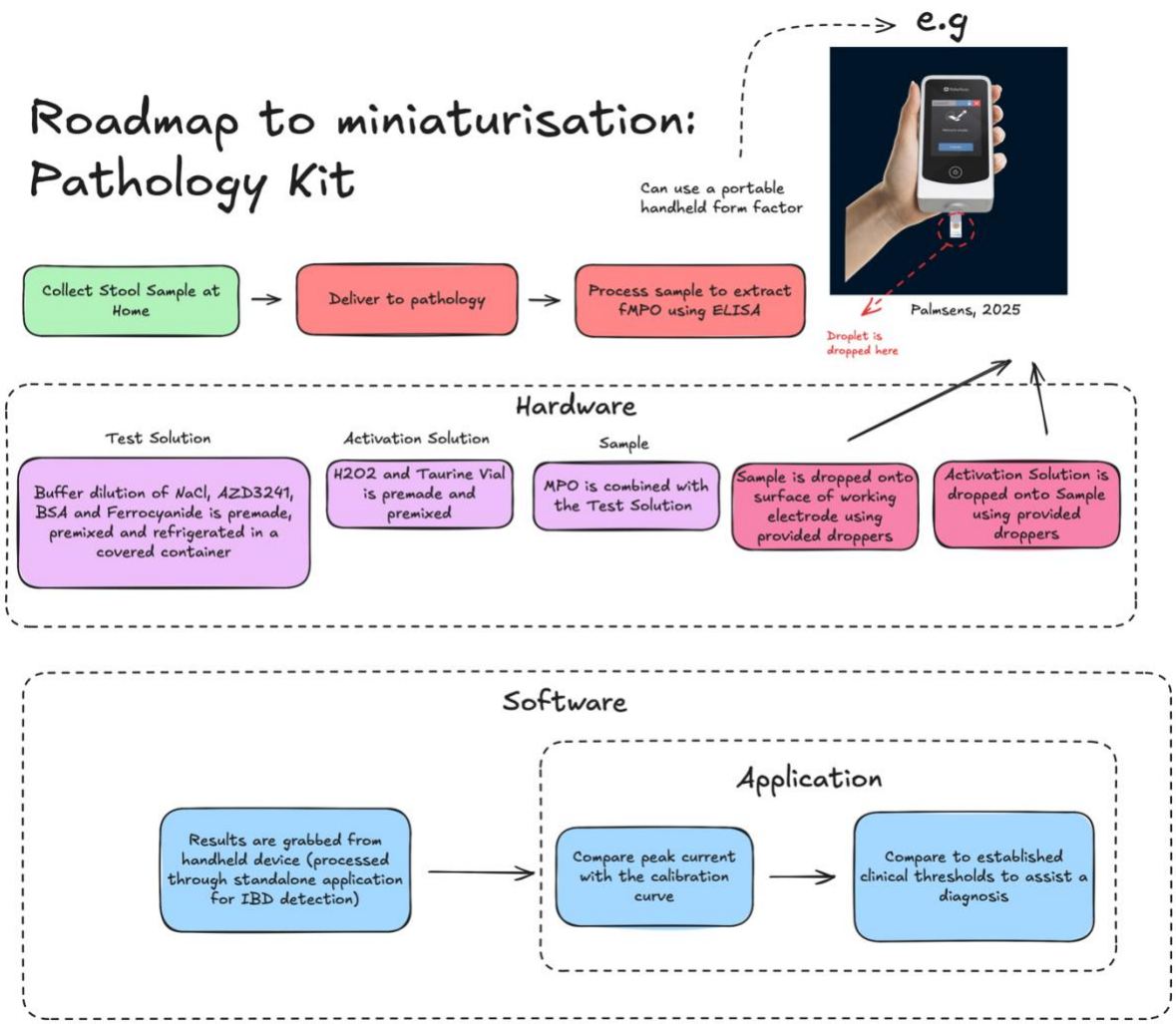

Figure 8. *Pathology Workflow*

4.2.3 In-home kit using IBDoc Hardware

The final step in the roadmap is a fully in-home kit, modelled on the class of smartphone-linked IVD home testing devices currently used for fecal calprotectin (fCal) monitoring, such as the IBDoc® platform [20]. This in-home implementation represents the endpoint of the miniaturisation roadmap and directly addresses Aim 2 by providing an electrochemical engineering pathway to miniaturised, home-use diagnostic equipment. These IVD home testing devices typically employ a screw-cap sampler with grooves that collect a fixed mass of stool and an integrated extraction chamber, giving patients a simple, closed system with controlled sample loading. In the proposed MPO device as shown by *Fig. 9 and 11*, this style of hardware is repurposed rather than reinvented. The sampling pin and grooves still trap a fixed stool mass, but

the main chamber is filled with an MPO-compatible extraction buffer instead of a calprotectin buffer to preserve enzyme activity. Downstream, throttled chambers and valves are redesigned so that, after the user twists or clicks through the numbered steps, the stool is eluted into the buffer, mixed with the test solution and then directed onto an integrated screen-printed electrode mounted in the base of the device. That electrode is pre-dosed with H_2O_2, taurine, AZD3241, BSA and ferrocyanide so that, by the time the sample arrives, all reagents required for MPO-driven TauCl formation and electrochemical detection are present without additional user metering. A neutralisation and absorption chamber at the bottom safely traps the spent reagent mixture and biological waste, quenching residual oxidants and supporting biosafety and household disposal requirements for home IVD kits while maintaining a closed, hygienic system.

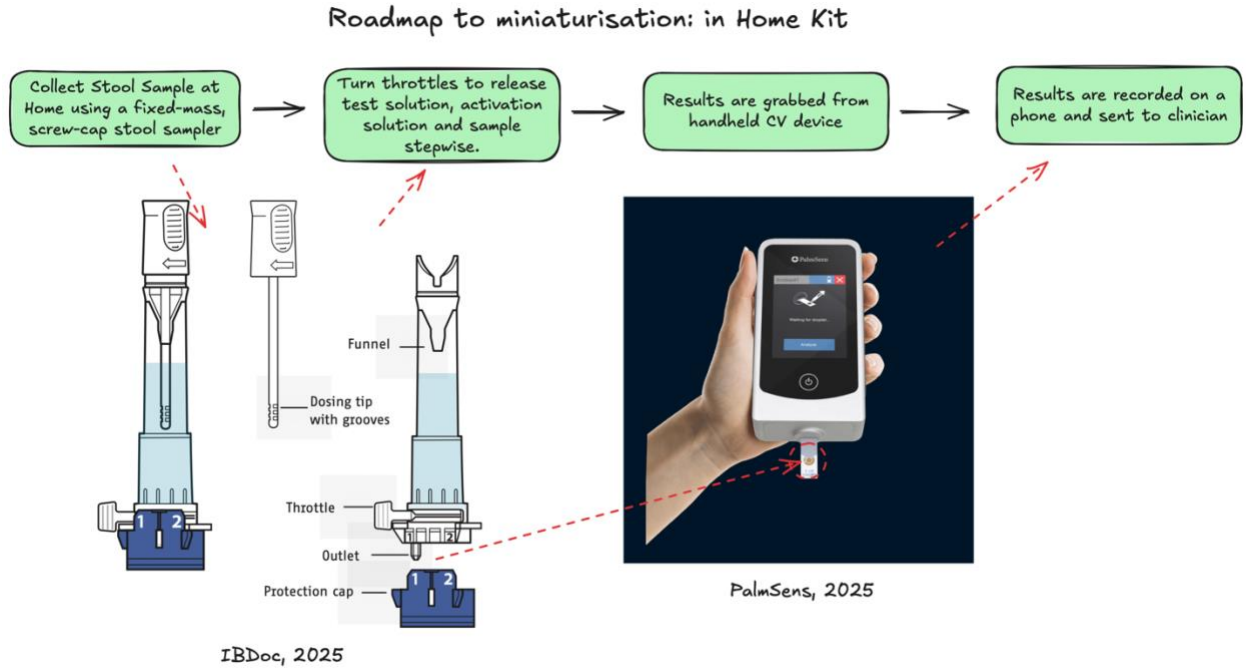

Figure 9. *In-home kit Workflow*

Critically, this choice of "off-the-shelf" IVD hardware is supported by published clinical data showing that fecal MPO and calprotectin track intestinal inflammation very closely. In a large patient cohort, fMPO concentrations correlated strongly with fCal across several orders of magnitude ($r \approx 0.82$, $p < 0.001$), and fMPO levels increased stepwise from remission through mild and moderate to severe disease as shown by *Fig 10*. These findings indicate that a device ecosystem already validated for calprotectin is also well suited to hosting an MPO read-out: the

same patient-friendly sampler and smartphone infrastructure can be retained while only the extraction buffer, on-cartridge chemistry and analytical target are changed. In other words, by exploiting the strong correlation between fCal and fMPO and reusing an established commercial platform, the proposed in-home kit reduces both engineering risk and adoption barriers, providing a realistic translational pathway from the electrochemical assay developed in this project to a clinically meaningful, patient-operated test.

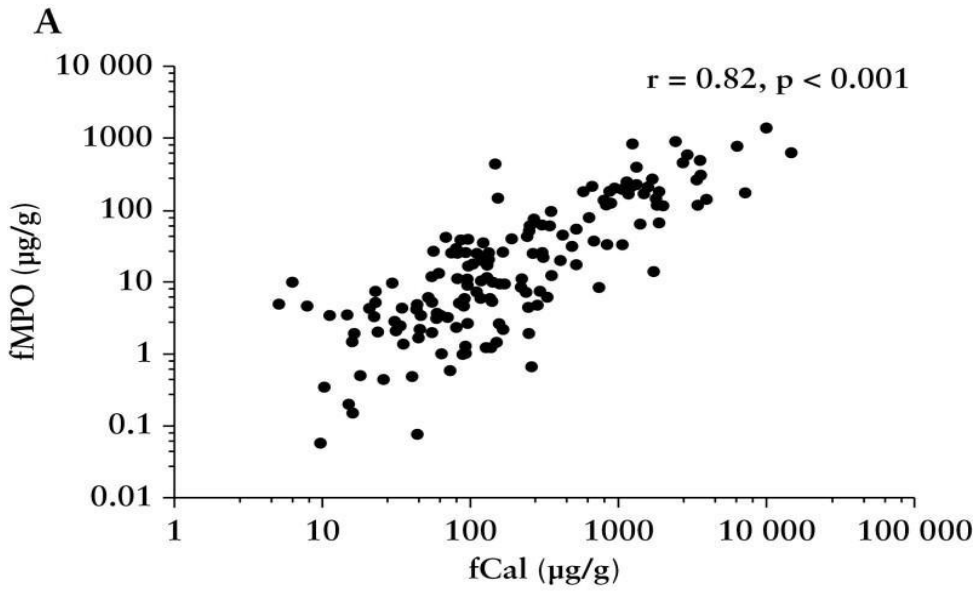

***Figure 10**. fCal vs fMPO correlation [33]*

To visualise how these functions could be implemented in a single patient-operated device, a prototype sketch of the proposed sampler was generated as shown by *Fig 11*. The design is based on IVD cartridges but incorporates additional chambers tailored to MPO electrochemistry. At the top, a screw-cap sampling pin with longitudinal grooves collects a fixed stool mass and is inserted into an MPO-compatible extraction buffer contained in the main reservoir. A funnel structure prevents back-splash and re-exit of biological material while the sample is agitated. Once extraction is complete, a rotary throttle is actuated to release the eluate into the lower section, where an integrated dropper delivers a defined volume onto a screen-printed electrode. This SPE is mounted externally so that it can dock with a portable potentiostat and is pre-dosed with H_2O_2, taurine, AZD3241 and BSA to initiate MPO-driven TauCl formation on contact with the sample. Beneath the reaction zone, neutralisation and absorption chambers immobilise residual oxidants

and biological waste, which are finally sealed by a protection cap. This sketch demonstrates that all steps of the benchtop assay sampling, extraction, reaction and safe disposal, can in principle be contained within a single, closed cartridge compatible with handheld electrochemical readout.

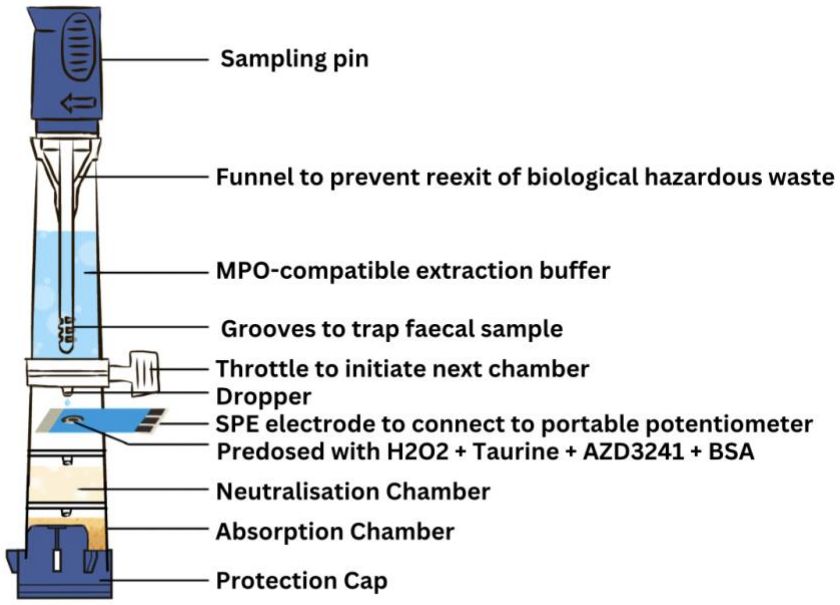

Figure 11. *Proposed Prototype sketch inspired by IVD systems*

4.2.4 Portable Potentiostats and Smartphone Application

Portable potentiostats are the enabling hardware across both the pathology and in-home workflows. Modern handheld potentiostats offer programmable CV protocols, nA–µA sensitivity, on-board data processing and either an integrated display or Bluetooth connection to a smartphone. In the pathology setting they function as compact bench instruments that can run the assay on disposable SPEs with minimal additional infrastructure [64], [65]. In the in-home kit, the same class of device can be docked to the base of the stool sampler (as illustrated), run a single CV scan, and transmit the processed result to a dedicated phone application. The app can store the calibration curve, convert peak current to estimated fMPO, present the patient with an intuitive traffic-light interpretation (remission, moderate, severe) [20], [33] and upload the result to the treating clinician. Together, these workflows show a realistic path from the current benchtop assay to a pathology-ready kit and, eventually, a patient-operated self-test built by repurposing proven IVD hardware for MPO rather than calprotectin.

Chapter 5: Discussion & Conclusion

The results chapter outlined a conceptual design for an at-home diagnostic device aimed at detecting inflammatory bowel disease (IBD) activity through biomarker analysis. This design incorporated several innovative features, including a sampling pin, MPO-compatible extraction buffer, and a multi-chamber system for sample processing and neutralization, all integrated with a screen-printed electrode (SPE) for connection to a portable potentiometer. These elements were intended to ensure safety, ease of use, and compatibility with electrochemical detection methods. Building on this conceptual framework, the discussion evaluates the potential impact of such a device on patient care and healthcare systems. Specifically, it considers the advantages of enabling non-invasive, home-based testing for IBD, such as improved accessibility, early detection, and reduced clinical burden. At the same time, this section critically examines the challenges associated with translating the design into a clinically validated product, including issues of analytical accuracy, regulatory compliance, and user adoption. By linking these considerations to the design features presented earlier, this discussion provides a roadmap for future development and implementation.

5.1 Summary of Principal Findings

This study shows that MPO activity can be transduced electrochemically by coupling the enzyme's halogenation cycle to HOCl-mediated oxidation of ferrocyanide. HOCl generated by MPO in the presence of chloride and H_2O_2 is rapidly trapped as TauCl, which then attenuates the ferri/ferrocyanide peak current in a predictable, dose-dependent way. By first building a chemical calibration curve with known HOCl/TauCl concentrations and then mapping MPO-driven signals onto that curve, the assay provides a functional read-out of oxidative MPO activity rather than just total protein mass. This directly addresses the gap highlighted by reviewing literature: current fMPO tests are largely ELISA-based, centralised in pathology laboratories, and slow, whereas there is a need for low-cost, activity-based, miniaturisable assays that can sit alongside or even replace existing calprotectin-only workflows and support real-time point-of-care monitoring and adhere to the STRIDE II guidelines. The proposed prototype sketch inspired by IVD systems as demonstrated in Fig 11. seems to be promising device that could be developed into a homebased device.

5.2 Potential Advantages of an At-Home IBD Testing Device

The development of a portable, user-friendly device for at-home testing of inflammatory bowel disease (IBD) biomarkers offers significant benefits for patient care and disease management. Such a device enhances convenience and accessibility, allowing patients to perform routine monitoring without the need for clinical visits. This is particularly advantageous for individuals in remote or underserved areas, reducing travel time and associated costs.

The device enables early detection and continuous monitoring of disease activity. Frequent, non-invasive testing can help identify flare-ups at an early stage, facilitating timely medical intervention and potentially improving long-term outcomes. By reducing reliance on invasive procedures such as colonoscopy for routine checks, the device also minimizes patient discomfort and clinical burden, freeing healthcare resources for more critical cases.
Safety considerations are integral to the design. Features such as a funnel to prevent re-exit of biological waste, a neutralization chamber, and a protection cap mitigate the risk of exposure to hazardous materials, ensuring hygienic handling. Furthermore, integration with portable potentiometers and digital platforms allows for real-time data acquisition and remote sharing with healthcare providers, supporting telemedicine and personalized treatment strategies. Finally, the device has the potential to be cost-effective, reducing overall healthcare expenditure by limiting hospital-based diagnostics and enabling proactive disease management.

5.3 Challenges and Limitations

Despite these advantages, several challenges must be addressed before such a device can be widely adopted. Analytical accuracy and reliability are essential if this device must demonstrate sensitivity and specificity comparable to laboratory-based assays to gain clinical acceptance. Variability in sample collection and handling by patients may introduce errors, necessitating robust design and clear user instructions.

Regulatory approval and standardisation represent another significant hurdle. Compliance with medical device regulations and validation through large-scale clinical trials will be essential to ensure safety and efficacy. Additionally, cost of development and manufacturing could impact

affordability, particularly if specialized reagents or sensors are required. User compliance and data privacy concerns also pose challenges. Patients must be willing and able to use the device correctly, and secure systems must be implemented for storing and transmitting health data. Finally, the device must be adaptable to biological variability among patients and account for potential interference from dietary or medication factors that could affect biomarker readings.

5.4 Interpretation of Assay Performance

Within that framework, the current work establishes proof-of-concept performance. The calibration data demonstrate a clear monotonic suppression of peak current with increasing HOCl/TauCl, and when enzymatic MPO experiments are overlaid onto this calibration, an LOD of 2.4 µM TauCl and an LOQ of 7.9 µM TauCl are obtained at 1 µg/mL MPO. Although preliminary, these values indicate that the ferrocyanide–TauCl system is sensitive enough to detect relatively small changes in oxidant production and, in principle, could be tuned to clinically relevant ranges. Coupled with the miniaturisation roadmap and the use of portable potentiostats, the work suggests a realistic route from benchtop chemistry to a hand-held device and even an at-home kit that reports MPO activity rather than only calprotectin.

A practical constraint throughout this work was the chemistry of HOCl itself. Neat HOCl is highly reactive, short-lived and difficult to handle reproducibly over the timescales of electrochemical experiments, especially when working with small volumes. For this reason, taurine was used to trap HOCl as TauCl, providing a more stable and dosable oxidant species for calibration. While this step was essential to obtain a controllable oxidant signal and to mimic the chloramine products expected in vivo, it introduced additional preparation, standardisation and waiting time for each experiment. In practice, the need to freshly generate and verify HOCl/TauCl batches on every run, and to re-optimise conditions when decay or side reactions occurred, slowed experimental throughput and limited how far the project could progress into more complex MPO and stool-matrix studies within the thesis timeframe.

5.3 Limitations and Sources of Uncertainty

Other constraints that could have been addressed in this experiment was that MPO concentration could have been systematically varied: all enzymatic experiments were performed at a single MPO level (1 µg/mL). As a result, the relationship between MPO activity and peak current was inferred

indirectly via the chemical HOCl/TauCl calibration, and true assay linearity, dynamic range and robustness to different enzyme loads remain undefined. The work was also conducted in controlled buffer systems rather than in real stool extracts, so matrix effects, interference from other oxidants or peroxidases, and the impact of endogenous antioxidants were not characterised. Finally, stability and repeatability (chip-to-chip variation, day-to-day drift, reagent shelf life) were not formally evaluated, meaning that the current data should be interpreted as feasibility rather than a final diagnostic specification.

5.4 Future Analytical and Clinical work

Future studies should first address these analytical gaps. A logical next step is to construct full calibration curves using multiple MPO concentrations and to express the response in conventional units of MPO activity, while continuing to use TauCl or HOCl surrogates as internal checks. Parallel measurements with reference ELISA or chemiluminescent assays would allow direct benchmarking of sensitivity, dynamic range and agreement.

Experiments in spiked and then genuine stool extracts are needed to quantify matrix effects, test selectivity against other stool components, and refine the extraction buffer and blocking strategy. On the electrochemical side, moving from CV to more sensitive techniques, studies conclude that DPV and SWV and exploring electrode modifications could improve LOD and reduce assay time, while systematic testing of reagent and sensor stability would support translation to a kit format [66], [67], [68].

5.5 Clinical Integration and Overall Significance

A further area worth discussing is clinical integration and usability. Because existing at-home IBD monitoring is built around calprotectin, it will be essential to understand how an MPO-activity read-out complements or augments current practice, whether as an earlier indicator of neutrophil activation, a companion marker that tracks response to therapy differently, or a fallback when calprotectin is equivocal. Human-factors work on the proposed sampler and portable potentiostat interface, together with health-economic analysis of decentralised MPO testing, will be needed to justify adoption.

In the context of device development, future work should focus on the development of a functional prototype based on the conceptual design that will allow for performance testing under real-world conditions. Rigorous validation studies, including large-scale clinical trials, will be necessary to establish sensitivity, specificity, and reproducibility compared to standard laboratory assays. And the integration with secure digital platforms will enable real-time data transmission, supporting telemedicine and personalized treatment strategies. Additional research should also explore cost optimisation, user training, and strategies to mitigate biological variability and interference from external factors. Collectively, these efforts will pave the way for transforming the conceptual design into a practical, patient-centered diagnostic tool.

5.6 Conclusion

This study investigated the feasibility of developing an at-home diagnostic solution for inflammatory bowel disease (IBD) by combining experimental analysis with conceptual design. Through a series of laboratory experiments, this study evaluated biomarker detection strategies and electrochemical sensing approaches suitable for non-invasive monitoring. The insights gained from these analyses informed the creation of a conceptual device.

This project provides an initial chemical and electrochemical foundation and a clear translational pathway, but substantial analytical validation and clinical correlation are the next critical steps before MPO-based electrochemical testing can realistically fill the gap identified in the literature.

References

[1] V. Kariyawasam *et al.*, "Myeloperoxidase Luminol Reaction – A Novel Faecal Assay for Predicting Colonoscopy Findings in Patients with Ulcerative Colitis: A Pilot Cross-Sectional Clinical Study," *Adv. Healthc. Mater.*, vol. n/a, no. n/a, p. e01825, doi: 10.1002/adhm.202501825.

[2] M. Lee and E. B. Chang, "Inflammatory Bowel Diseases (IBD) and the Microbiome-Searching the Crime Scene for Clues," *Gastroenterology*, vol. 160, no. 2, pp. 524–537, Jan. 2021, doi: 10.1053/j.gastro.2020.09.056.

[3] "Diagnosis and management of inflammatory bowel disease - Li - 2024 - Journal of Evidence-Based Medicine - Wiley Online Library." Accessed: May 30, 2025. [Online]. Available: https://onlinelibrary.wiley.com/doi/10.1111/jebm.12626

[4] B. Caron, S. Honap, and L. Peyrin-Biroulet, "Epidemiology of Inflammatory Bowel Disease across the Ages in the Era of Advanced Therapies," *J. Crohns Colitis*, vol. 18, no. Suppl 2, pp. ii3–ii15, Oct. 2024, doi: 10.1093/ecco-jcc/jjae082.

[5] S. J. Kwon, M. S. Khan, and S. G. Kim, "Intestinal Inflammation and Regeneration-Interdigitating Processes Controlled by Dietary Lipids in Inflammatory Bowel Disease," *Int. J. Mol. Sci.*, vol. 25, no. 2, p. 1311, Jan. 2024, doi: 10.3390/ijms25021311.

[6] C. McDowell, U. Farooq, and M. Haseeb, "Inflammatory Bowel Disease," in *StatPearls*, Treasure Island (FL): StatPearls Publishing, 2025. Accessed: Nov. 16, 2025. [Online]. Available: http://www.ncbi.nlm.nih.gov/books/NBK470312/

[7] "Clinical features and oncological outcomes of intestinal cancers associated with ulcerative colitis and Crohn's disease | Journal of Gastroenterology." Accessed: May 30, 2025. [Online]. Available: https://link.springer.com/article/10.1007/s00535-022-01927-y

[8] Z. Cai, S. Wang, and J. Li, "Treatment of Inflammatory Bowel Disease: A Comprehensive Review," *Front. Med.*, vol. 8, p. 765474, 2021, doi: 10.3389/fmed.2021.765474.

[9] N. Jayasooriya *et al.*, "Systematic review with meta-analysis: Time to diagnosis and the impact of delayed diagnosis on clinical outcomes in inflammatory bowel disease," *Aliment. Pharmacol. Ther.*, vol. 57, no. 6, pp. 635–652, 2023, doi: 10.1111/apt.17370.

[10] S. A. Rizo-Téllez, M. Sekheri, and J. G. Filep, "Myeloperoxidase: Regulation of Neutrophil Function and Target for Therapy," *Antioxidants*, vol. 11, no. 11, Art. no. 11, Nov. 2022, doi: 10.3390/antiox11112302.

[11] A. dos Santos Ramos, G. C. S. Viana, M. de Macedo Brigido, and J. F. Almeida, "Neutrophil extracellular traps in inflammatory bowel diseases: Implications in pathogenesis and therapeutic targets," *Pharmacol. Res.*, vol. 171, p. 105779, Sep. 2021, doi: 10.1016/j.phrs.2021.105779.

[12] Y. Naito, T. Takagi, and T. Yoshikawa, "Molecular fingerprints of neutrophil-dependent oxidative stress in inflammatory bowel disease," *J. Gastroenterol.*, vol. 42, no. 10, pp. 787–798, Oct. 2007, doi: 10.1007/s00535-007-2096-y.

[13] D. De Deo *et al.*, "Digital biomarkers and artificial intelligence: a new frontier in personalized management of inflammatory bowel disease," *Front. Immunol.*, vol. 16, Aug. 2025, doi: 10.3389/fimmu.2025.1637159.

[14] I. Grishkovskaya *et al.*, "Structure of human promyeloperoxidase (proMPO) and the role of the propeptide in processing and maturation," *J. Biol. Chem.*, vol. 292, no. 20, pp. 8244–8261, May 2017, doi: 10.1074/jbc.M117.775031.

[15] "UniProt," P05164 PERM_HUMAN. Accessed: Nov. 16, 2025. [Online]. Available: https://www.uniprot.org/uniprotkb/P05164/entry
[16] "Halogenation and peroxidase cycle of MPO. MPO reacts with H2O2 to form...," ResearchGate. Accessed: Nov. 14, 2025. [Online]. Available: https://www.researchgate.net/figure/Halogenation-and-peroxidase-cycle-of-MPO-MPO-reacts-with-H2O2-to-form-compound-I-which_fig2_227858206
[17] N. H. Nguyen *et al.*, "Digital Health Technologies for Remote Monitoring and Management of Inflammatory Bowel Disease: A Systematic Review," *Off. J. Am. Coll. Gastroenterol. ACG*, vol. 117, no. 1, p. 78, Jan. 2022, doi: 10.14309/ajg.0000000000001545.
[18] M. Goren *et al.*, "P0267 Proactive Remote Monitoring of Inflammatory Bowel Disease for Improved Outcomes and Flare Prediction," *J. Crohns Colitis*, vol. 19, no. Supplement_1, pp. i701–i702, Jan. 2025, doi: 10.1093/ecco-jcc/jjae190.0441.
[19] D. Turner *et al.*, "STRIDE-II: An Update on the Selecting Therapeutic Targets in Inflammatory Bowel Disease (STRIDE) Initiative of the International Organization for the Study of IBD (IOIBD): Determining Therapeutic Goals for Treat-to-Target strategies in IBD," *Gastroenterology*, vol. 160, no. 5, pp. 1570–1583, Apr. 2021, doi: 10.1053/j.gastro.2020.12.031.
[20] "About IBDoc® | BÜHLMANN | Calprotectin Home Test." Accessed: Nov. 16, 2025. [Online]. Available: https://www.ibdoc.net/about-ibdoc-2/
[21] K. Ina *et al.*, "Increased mucosal production of granulocyte colony-stimulating factor is related to a delay in neutrophil apoptosis in Inflammatory Bowel disease," *J. Gastroenterol. Hepatol.*, vol. 14, no. 1, pp. 46–53, Jan. 1999, doi: 10.1046/j.1440-1746.1999.01807.x.
[22] D. R. Hansberry, K. Shah, P. Agarwal, and N. Agarwal, "Fecal Myeloperoxidase as a Biomarker for Inflammatory Bowel Disease," *Cureus*, vol. 9, no. 1, p. e1004, doi: 10.7759/cureus.1004.
[23] G. P. Ramos and K. A. Papadakis, "Mechanisms of Disease: Inflammatory Bowel Diseases," *Mayo Clin. Proc.*, vol. 94, no. 1, pp. 155–165, Jan. 2019, doi: 10.1016/j.mayocp.2018.09.013.
[24] M. Ortega-Zapero, R. Gomez-Bris, I. Pascual-Laguna, A. Saez, and J. M. Gonzalez-Granado, "Neutrophils and NETs in Pathophysiology and Treatment of Inflammatory Bowel Disease," *Int. J. Mol. Sci.*, vol. 26, no. 15, p. 7098, Jul. 2025, doi: 10.3390/ijms26157098.
[25] T. Chen, J. Liu, R. Hang, Q. Chen, and D. Wang, "Neutrophils: From Inflammatory Bowel Disease to Colitis-Associated Colorectal Cancer," *J. Inflamm. Res.*, vol. 18, pp. 925–947, 2025, doi: 10.2147/JIR.S497701.
[26] "(PDF) Clinical Comparison of OC-Sensor Pledia and Phadia 250 for Fecal Calprotectin Testing." Accessed: Jun. 02, 2025. [Online]. Available: https://www.researchgate.net/publication/385636927_Clinical_Comparison_of_OC-Sensor_Pledia_and_Phadia_250_for_Fecal_Calprotectin_Testing
[27] T. Rokkas, P. Portincasa, and I. E. Koutroubakis, "Fecal calprotectin in assessing inflammatory bowel disease endoscopic activity: a diagnostic accuracy meta-analysis," *J. Gastrointest. Liver Dis. JGLD*, vol. 27, no. 3, pp. 299–306, Sep. 2018, doi: 10.15403/jgld.2014.1121.273.pti.
[28] J. Langhorst, J. Boone, R. Lauche, A. Rueffer, and G. Dobos, "Faecal Lactoferrin, Calprotectin, PMN-elastase, CRP, and White Blood Cell Count as Indicators for Mucosal Healing and Clinical Course of Disease in Patients with Mild to Moderate Ulcerative Colitis:

Post Hoc Analysis of a Prospective Clinical Trial," *J. Crohns Colitis*, vol. 10, no. 7, pp. 786–794, Jul. 2016, doi: 10.1093/ecco-jcc/jjw044.
[29] B. S. Witarto, V. Visuddho, A. P. Witarto, M. T. A. Sampurna, and A. Irzaldy, "Performance of fecal S100A12 as a novel non-invasive diagnostic biomarker for pediatric inflammatory bowel disease: a systematic review and meta-analysis," *J. Pediatr. (Rio J.)*, vol. 99, no. 5, pp. 432–442, 2023, doi: 10.1016/j.jped.2023.03.002.
[30] A. Heida, A. C. M. Kobold, L. Wagenmakers, K. van de Belt, and P. F. van Rheenen, "Reference values of fecal calgranulin C (S100A12) in school aged children and adolescents," *Clin. Chem. Lab. Med.*, vol. 56, no. 1, pp. 126–131, Nov. 2017, doi: 10.1515/cclm-2017-0152.
[31] A. Swaminathan *et al.*, "Comparison of Fecal Calprotectin and Myeloperoxidase in Predicting Outcomes in Inflammatory Bowel Disease," *Inflamm. Bowel Dis.*, vol. 31, no. 1, pp. 28–36, Jan. 2025, doi: 10.1093/ibd/izae032.
[32] M. Di Ruscio, F. Vernia, A. Ciccone, G. Frieri, and G. Latella, "Surrogate Fecal Biomarkers in Inflammatory Bowel Disease: Rivals or Complementary Tools of Fecal Calprotectin?," *Inflamm. Bowel Dis.*, vol. 24, no. 1, pp. 78–92, Dec. 2017, doi: 10.1093/ibd/izx011.
[33] A. Swaminathan *et al.*, "Faecal Myeloperoxidase as a Biomarker of Endoscopic Activity in Inflammatory Bowel Disease," *J. Crohns Colitis*, vol. 16, no. 12, pp. 1862–1873, Jul. 2022, doi: 10.1093/ecco-jcc/jjac098.
[34] A. L. Schroder *et al.*, "Neutrophil Extracellular Trap Density Increases With Increasing Histopathological Severity of Crohn's Disease," *Inflamm. Bowel Dis.*, vol. 28, no. 4, pp. 586–598, Mar. 2022, doi: 10.1093/ibd/izab239.
[35] P. Avery, J. Adio, R. Cornford, and L. Younge, "N24 At Home Calprotectin a United Kingdom Patient Perspectives and Tertiary Center Experience," *J. Crohns Colitis*, vol. 17, no. Supplement_1, pp. i1052–i1053, Feb. 2023, doi: 10.1093/ecco-jcc/jjac190.1083.
[36] S.-C. Wei, C.-C. Tung, M.-T. Weng, and J.-M. Wong, "Experience of patients with inflammatory bowel disease in using a home fecal calprotectin test as an objective reported outcome for self-monitoring," *Intest. Res.*, vol. 16, no. 4, pp. 546–553, Oct. 2018, doi: 10.5217/ir.2018.00052.
[37] A. Thomas, M. Clarke, V. Cairns, J. Goodhand, T. Ahmad, and N. Kennedy, "P355 Diagnostic accuracy and usability of home calprotectin testing," *J. Crohns Colitis*, vol. 13, no. Supplement_1, p. S281, Jan. 2019, doi: 10.1093/ecco-jcc/jjy222.479.
[38] J.-T. Shi, Y. Zhang, Y. She, H. Goyal, Z.-Q. Wu, and H.-G. Xu, "Diagnostic Utility of Non-invasive Tests for Inflammatory Bowel Disease: An Umbrella Review," *Front. Med.*, vol. 9, p. 920732, 2022, doi: 10.3389/fmed.2022.920732.
[39] "High-performance H 2 sensor based on Polyaniline-WO 3 nanocomposite for portable batteries and breathomics-diagnosis of irritable bowel syndrome | Request PDF," *ResearchGate*, Dec. 2024, doi: 10.1016/j.ijhydene.2023.08.151.
[40] M. Goebel-Stengel, A. Stengel, M. Schmidtmann, I. van der Voort, P. Kobelt, and H. Mönnikes, "Unclear Abdominal Discomfort: Pivotal Role of Carbohydrate Malabsorption," *J. Neurogastroenterol. Motil.*, vol. 20, no. 2, pp. 228–235, Apr. 2014, doi: 10.5056/jnm.2014.20.2.228.
[41] "Non-invasive continuous real-time in vivo analysis of microbial hydrogen production shows adaptation to fermentable carbohydrates in mice | Scientific Reports." Accessed: Jun. 04, 2025. [Online]. Available: https://www.nature.com/articles/s41598-018-33619-0

[42] M. Nishibori, W. Shin, N. Izu, T. Itoh, and I. Matsubara, “Sensing performance of thermoelectric hydrogen sensor for breath hydrogen analysis,” *Sens. Actuators B Chem.*, vol. 137, no. 2, pp. 524–528, Apr. 2009, doi: 10.1016/j.snb.2009.01.029.
[43] R. Slater *et al.*, “Gas Chromatography-Sensor System Aids Diagnosis of Inflammatory Bowel Disease, and Separates Crohn’s from Ulcerative Colitis, in Children,” *Sensors*, vol. 24, no. 15, p. 5079, Aug. 2024, doi: 10.3390/s24155079.
[44] S. Bosch *et al.*, “The influence of lifestyle factors on fecal volatile organic compound composition as measured by an electronic nose,” *J. Breath Res.*, vol. 13, no. 4, p. 046001, Jun. 2019, doi: 10.1088/1752-7163/ab2775.
[45] “P004 Untargeted serum metabolome shows Crohn Disease (CD) associated signature, signals that correlate with disease activity and CRP, and signals that may precede disease flare | Journal of Crohn’s and Colitis | Oxford Academic.” Accessed: Jun. 04, 2025. [Online]. Available: https://academic.oup.com/ecco-jcc/article/17/Supplement_1/i173/7009453
[46] P. A. Thwaites, R. Slater, C. Probert, and P. R. Gibson, “Recent advances in measuring the effects of diet on gastrointestinal physiology: Sniffing luminal gases and fecal volatile organic compounds,” *JGH Open*, vol. 8, no. 8, p. e70006, 2024, doi: 10.1002/jgh3.70006.
[47] Y. A. Al Naam, S. Elsafi, M. H. Al Jahdali, R. S. Al Shaman, B. H. Al-Qurouni, and E. M. Al Zahrani, “The Impact of Total Automaton on the Clinical Laboratory Workforce: A Case Study,” *J. Healthc. Leadersh.*, vol. 14, pp. 55–62, May 2022, doi: 10.2147/JHL.S362614.
[48] G. P. Caviglia, D. G. Ribaldone, C. Rosso, G. M. Saracco, M. Astegiano, and R. Pellicano, “Fecal calprotectin: beyond intestinal organic diseases,” *Panminerva Med.*, vol. 60, no. 1, pp. 29–34, Mar. 2018, doi: 10.23736/S0031-0808.18.03405-5.
[49] D. Fitzgerald, K. Sugrue, J. McCarthy, and M. Buckley, “N804 An evaluation of patient satisfaction with IBDoc calprotectin home test system,” *J. Crohns Colitis*, vol. 11, no. suppl_1, p. S493, Feb. 2017, doi: 10.1093/ecco-jcc/jjx002.928.
[50] A. C. Moore *et al.*, “IBDoc Canadian User Performance Evaluation,” *Inflamm. Bowel Dis.*, vol. 25, no. 6, pp. 1107–1114, May 2019, doi: 10.1093/ibd/izy357.
[51] “Agreement Between Home-Based Measurement of Stool Calprotectin and ELISA Results for Monitoring Inflammatory Bowel Disease Activity - Clinical Gastroenterology and Hepatology.” Accessed: Nov. 16, 2025. [Online]. Available: https://www.cghjournal.org/article/S1542-3565(17)30712-7/fulltext
[52] X. Xu, G. Li, L. Xue, S. Dong, J. Luo, and Z. Cao, “Microfluidic devices integrated with plasmonic nanostructures for sensitive fluorescent immunoassays,” *Biomicrofluidics*, vol. 18, no. 1, p. 011303, Feb. 2024, doi: 10.1063/5.0174653.
[53] P. Nath, K. R. Mahtaba, A. Ray, P. Nath, K. R. Mahtaba, and A. Ray, “Fluorescence-Based Portable Assays for Detection of Biological and Chemical Analytes,” *Sensors*, vol. 23, no. 11, May 2023, doi: 10.3390/s23115053.
[54] T. Davis, “Novel Method for Quantifying Faecal Myeloperoxidase in Patients with Inflammatory Bowel Disease,” Nov. 2024.
[55] E. Sciurti *et al.*, “Label-free electrochemical biosensor for direct detection of Oncostatin M (OSM) inflammatory bowel diseases (IBD) biomarker in human serum,” *Talanta*, vol. 271, p. 125726, May 2024, doi: 10.1016/j.talanta.2024.125726.
[56] J. Hoyo, A. Bassegoda, and T. Tsanov, “Electrochemical quantification of biomarker myeloperoxidase”.

[57] R. Nandeshwar and S. Tallur, “Electrochemical detection of myeloperoxidase (MPO) in blood plasma with surface-modified electroless nickel immersion gold (ENIG) printed circuit board (PCB) electrodes,” *Biosens. Bioelectron.*, vol. 246, p. 115891, Feb. 2024, doi: 10.1016/j.bios.2023.115891.
[58] T. Y *et al.*, “Flexible Amperometric Immunosensor Based on Colloidal Quantum Dots for Detecting the Myeloperoxidase (MPO) Systemic Inflammation Biomarker,” *Biosensors*, vol. 13, no. 2, Feb. 2023, doi: 10.3390/bios13020255.
[59] M. C. Valdivieso, L. Ortiz, and J. J. Castillo, “Myeloperoxidase as a biomarker in periodontal disease: electrochemical detection using printed screen graphene electrodes,” *Odontology*, Feb. 2025, doi: 10.1007/s10266-024-01043-8.
[60] J. Kim *et al.*, “High-quantum yield alloy-typed core/shell CdSeZnS/ZnS quantum dots for bio-applications,” *J. Nanobiotechnology*, vol. 20, no. 1, p. 22, Jan. 2022, doi: 10.1186/s12951-021-01227-2.
[61] H. Abouali *et al.*, “A Bead-Based Quantum Dot Immunoassay Integrated with Multi-Module Microfluidics Enables Real-Time Multiplexed Detection of Blood Insulin and Glucagon,” *Adv. Sci.*, vol. 12, no. 29, p. 2412185, 2025, doi: 10.1002/advs.202412185.
[62] R. Zhou *et al.*, “The Enhanced Sensitivity of a Porous Silicon Microcavity Biosensor Based on an Angular Spectrum Using CdSe/ZnS Quantum Dots,” *Sensors*, vol. 19, no. 22, Nov. 2019, doi: 10.3390/s19224872.
[63] “EmStat4T,” PalmSens. Accessed: Nov. 16, 2025. [Online]. Available: https://www.palmsens.com/emstat4t/
[64] R. Setiyono *et al.*, “UnpadStat Design: Portable Potentiostat for Electrochemical Sensing Measurements Using Screen Printed Carbon Electrode,” *Micromachines*, vol. 14, no. 2, Jan. 2023, doi: 10.3390/mi14020268.
[65] D. Snizhko, Y. Zholudov, A. Kukoba, and G. Xu, “Potentiostat design keys for analytical applications,” *J. Electroanal. Chem.*, vol. 936, p. 117380, May 2023, doi: 10.1016/j.jelechem.2023.117380.
[66] A. E. T. Ahmed *et al.*, “AI-optimized electrochemical aptasensors for stable, reproducible detection of neurodegenerative diseases, cancer, and coronavirus,” *Heliyon*, vol. 11, no. 1, Jan. 2025, doi: 10.1016/j.heliyon.2024.e41338.
[67] P. M. Jahani, M. Jafari, and F. N. Ravari, “CuFe2O4 nanoparticles-based electrochemical sensor for sensitive determination of the anticancer drug 5-fluorouracil,” *ADMET DMPK*, vol. 11, no. 2, pp. 201–210, Jun. 2023, doi: 10.5599/admet.1691.
[68] A. Shaver and N. Arroyo-Currás, “The challenge of long-term stability for nucleic acid-based electrochemical sensors,” *Curr. Opin. Electrochem.*, vol. 32, p. 100902, Apr. 2022, doi: 10.1016/j.coelec.2021.100902.

Appendix 1. Range of concentrations (50 µM, 500 µM, and 5 mM) tested to identify the optimal condition. Control of HOCl impact on PBS (10mM).

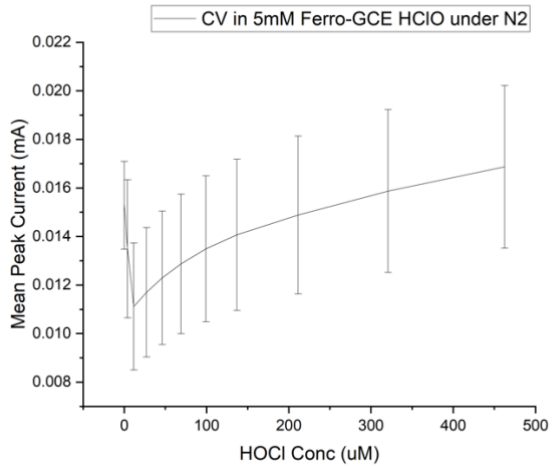

Effect of HOCl Conc. on Ferrocyanide ($5mM$) in N_2 purged conditions

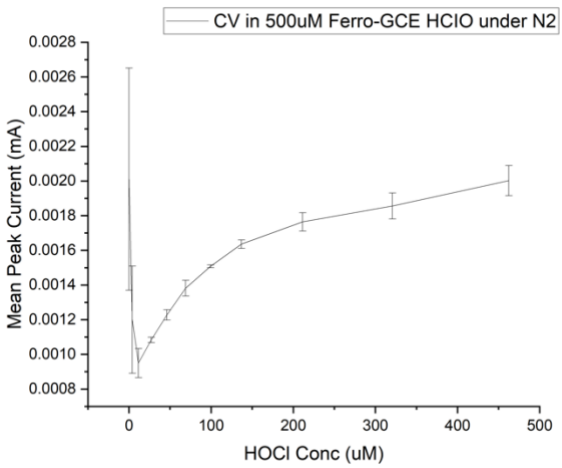

Effect of HOCl Conc. on Ferrocyanide ($500\mu M$) in N_2 purged conditions

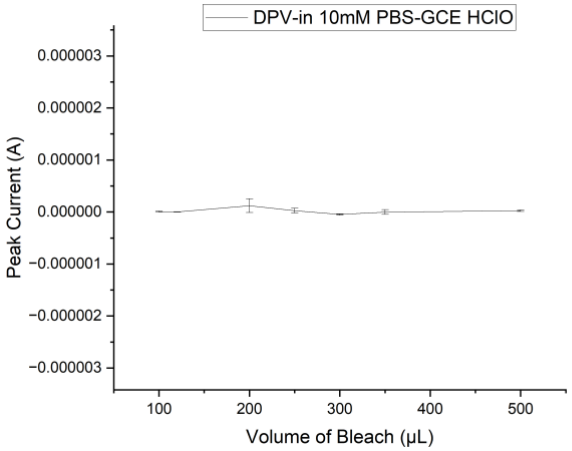

Effect of HOCl Conc. on PBS ($10mM$)

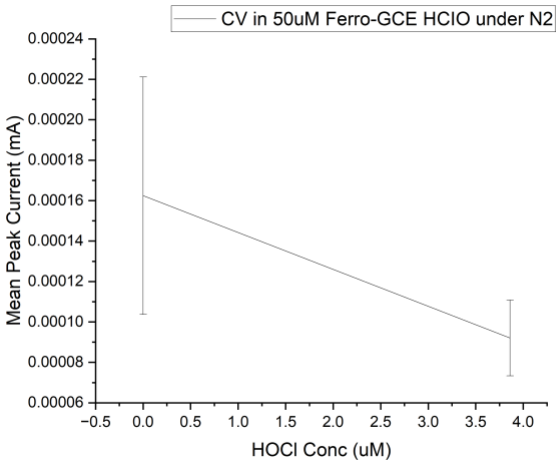

Effect of HOCl Conc. on Ferrocyanide ($50\mu M$) in N_2 purged conditions

Appendix 2. MATLAB Code to Extract peaks

```
clear; clc; close all;


Trials = [1, 2, 3];
```

```
Volumes = [0 5 10 20 25 30 40 50 100 150 200];
Concentrations = [0.00 3.86 11.57 26.96 46.12 69.01 99.35 137.00 211.37 320.68 462.40]; % µM

FileName = 'SUMMARY.xlsx';
TOTAL    = length(Trials) * length(Volumes);
r        = 0;

% Preallocate SUMMARY so we can fill it inside the loop
% Columns: [Volume, Conc, Ep_peak (mV), Ip_peak (mA), dIP (%), I/I0, dIP (µA)]
SUMMARY = zeros(TOTAL, 7);

for i = 1:length(Trials)
      SUMMARY = [];
      for j = 1:length(Volumes)
         % Generate the filename for this iteration
         fname = sprintf('SPE-CV-%duL Bleach-12mL Potassium Ferro under N2 (5mM) T%d_01',
Volumes(j), Trials(i));
         %Rename SPE-CV-%duL...(500uM, 50uM)

         % Read data from the specified Excel file
         DATA = readmatrix(fname, 'Sheet', 'DCData1');
         A    = find(DATA(:,5) == 3);
         E    = DATA(A,10);   % Third-cycle potentials (V)
         I    = DATA(A, 9);   % Third-cycle currents   (A)

         % Convert raw data to mV and mA for plotting
         E_mV = E * 1e3;  % mV
         I_mA = I * 1e3;  % mA

         % Plot raw data (mV vs. mA)
         figure;
         subplot(1,3,1);
         plot(E_mV, I_mA);
```

```
xlabel('Potential (mV)');
ylabel('Current (mA)');
title('Raw Data');

% Truncate after max(E) (in volts), then update mV/mA arrays
idxMax = find(E == max(E), 1, 'first');
E(idxMax:end)    = [];
I(idxMax:end)    = [];
E_mV(idxMax:end) = [];
I_mA(idxMax:end) = [];

% Filter to E ≥ 0 V
idxKeep = (E >= 0);
E    = E(idxKeep);
I    = I(idxKeep);
E_mV = E_mV(idxKeep);
I_mA = I_mA(idxKeep);

subplot(1,3,2);
plot(E_mV, I_mA);
xlabel('Potential (mV)');
ylabel('Current (mA)');
title('Filtered Data');

% Linear background fit on region E > 0.6 V
t  = find(E > 0.6);
Ix = min(I(t));        % minimum current in region E > 0.6 (A)
Ex = E(I == Ix);       % corresponding potential (V)
a  = (Ix - I(1)) / (Ex - E(1));
b  = I(1) - a * E(1);

% Compute background line in original units, then convert for plotting
L    = a .* E + b;   % background current (A)
```

```
L_mA  = L * 1e3;      % background current (mA)
Ic    = I - L;        % corrected current (A)
Ic_mA = Ic * 1e3;     % corrected current (mA)

hold on;
plot(E_mV, L_mA, '--r');  % plot background line in mA

subplot(1,3,3);
plot(E_mV, Ic_mA);
xlabel('Potential (mV)');
ylabel('Corrected Current (mA)');
title('Corrected Current');

% Find the peak of Ic (in A) and convert to mA
[IcMax_A, pIdx] = max(Ic);     % peak current in A
IcMax_mA        = IcMax_A * 1e3;   % peak current in mA
Ep_peak_V       = E(pIdx);         % potential at peak (V)
Ep_peak_mV      = Ep_peak_V * 1e3;  % potential at peak (mV)

% Mark the peak on the “Corrected Current” plot
hold on;
plot(E_mV(pIdx), Ic_mA(pIdx), 'ro', 'MarkerFaceColor','r');

if j == 1
   IcMax_ref_A = IcMax_A;  % reference peak in A for j = 1
end

% Compute metrics (using amps internally)
dIP_percent = 100 * ((IcMax_A - IcMax_ref_A) / IcMax_ref_A);
I_ratio     = IcMax_A / IcMax_ref_A;
dIP_uA      = 1e6 * (IcMax_A - IcMax_ref_A);  % difference in µA

% Store into SUMMARY (converted to mV/mA where appropriate)
```

```
    SUMMARY(j, :) = [
        Volumes(j), ...
        Concentrations(j), ...
        Ep_peak_mV, ...   % mV
        IcMax_mA,   ...   % mA
        dIP_percent, ...
        I_ratio, ...
        dIP_uA ...
    ];

    % Update and display progress, then print Ex and Ix in mV/mA
    r = r + 1;
    clc;
    disp([num2str(r), '/', num2str(TOTAL)]);
    fprintf('    Ex = %.1f mV\tIx = %.4f mA\n', Ex*1e3, Ix*1e3);
    fprintf('    Ep_peak = %.1f mV\tIcMax = %.4f mA\n', Ep_peak_mV, IcMax_mA);

    % Optionally close the figure to avoid too many open windows
    % close(gcf);
end


        % Define column titles
        Titles = {
            'Droplet size (uL)', ...
            'HOCl Conc (uM)', ...
            'Ep_peak (mV)', ...
            'Ip_peak (mA)', ...
            'dIP (%)', ...
            'I/I0', ...
            'dIP (µA)'
        };

        % Write titles and data to the 'Summary' sheet
```

```
    writecell(Titles, FileName, 'Sheet', sprintf('T%d', Trials(i)), 'Range', 'F6:L6');
    writematrix(SUMMARY, FileName, 'Sheet', sprintf('T%d', Trials(i)), 'Range', 'F7:L17');
end
```